Technical Report Documentation Page

1. Report No. FHWA/TX-06/0-4357-1	2. Government Accession No.	3. Recipient's Catalog No.
4. Title and Subtitle IMPROVED TESTING SPEED OF THE ROLLING DYNAMIC DEFLECTOMETER		5. Report Date November 2005; Revised February 2006
		6. Performing Organization Code
7. Author(s) Jeffrey L. Lee and Kenneth H. Stokoe, II		8. Performing Organization Report No. 0-4357-1
9. Performing Organization Name and Address Center for Transportation Research The University of Texas at Austin 3208 Red River, Suite 200 Austin, TX 78705-2650		10. Work Unit No. (TRAIS)
		11. Contract or Grant No. 0-4357
12. Sponsoring Agency Name and Address Texas Department of Transportation Research and Technology Implementation Office P.O. Box 5080 Austin, TX 78763-5080		13. Type of Report and Period Covered Technical Report March 2002–November 2005
		14. Sponsoring Agency Code

15. Supplementary Notes

Project performed in cooperation with the Texas Department of Transportation and the Federal Highway Administration.

Project Title: Further Development of the Rolling Dynamic Deflectometer to Increase Test Speed

16. Abstract

The Rolling Dynamic Deflectometer (RDD) was developed by the researchers at The University of Texas at Austin in the late 1990s. It has been used in many project-level pavement studies in Texas. The current testing speed of the RDD is limited to 1 mph (1.6 km/hr) using first-generation rolling sensors. This TxDOT research project 0-4357 was initiated to further develop the RDD. The primary objective of this project is to design and build second-generation rolling sensors, which will triple the current RDD testing speed from 1 mph (1.6 km/hr) to 3 mph (4.8 km/hr).

Four second-generation rolling sensors were designed, built and calibrated in the laboratory. Based on the results collected during two field trials at the Pickle Research Campus, it was found that the second-generation rolling sensors can readily achieve the testing speed of 3 mph (4.8 km/hr). In terms of rolling noise characteristics, this new rolling sensor has lower rolling noise than the first-generation rolling sensor.

17. Key Words	18. Distribution Statement
Rolling Dynamic Deflectometer (RDD), pavement testing, highway pavement testing, deflection testing, nondestructive testing	No restrictions. This document is available to the public through the National Technical Information Service, Springfield, Virginia 22161; www.ntis.gov.

19. Security Classif. (of report)	20. Security Classif. (of this page)	21. No. of pages	22. Price
Unclassified	Unclassified	86	

Form DOT F 1700.7 (8-72)   Reproduction of completed page authorized

Improved Testing Speed of the Rolling Dynamic Deflectometer

Jeffrey L. Lee
Kenneth H. Stokoe, II

CTR Technical Report:	0-4357-1
Report Date:	November 2005; Revised February 2006
Research Project:	0-4357
Research Project Title:	Further Development of the Rolling Dynamic Deflectometer to Increase Test Speed
Sponsoring Agency:	Texas Department of Transportation
Performing Agency:	Center for Transportation Research at The University of Texas at Austin

Project performed in cooperation with the Texas Department of Transportation and the Federal Highway Administration.

Center for Transportation Research
The University of Texas at Austin
3208 Red River
Austin, TX 78705

www.utexas.edu/research/ctr

Printed in the United States of America

Disclaimers

Author's Disclaimer: The contents of this report reflect the views of the authors, who are responsible for the facts and the accuracy of the data presented herein. The contents do not necessarily reflect the official view or policies of the Federal Highway Administration or the Texas Department of Transportation (TxDOT). This report does not constitute a standard, specification, or regulation.

Engineering Disclaimer

NOT INTENDED FOR CONSTRUCTION, BIDDING, OR PERMIT PURPOSES.

Project Engineer: Kenneth H. Stokoe, II
Professional Engineer License State and Number: Texas No. 49095

Acknowledgments

The success of this project was made possible only through the cooperation and the assistance of a number of dedicated people. Technical staff from The University of Texas at Austin carried out much of the construction of the new rolling sensor. Mr. Larry Larson of the Central Machine Shop was responsible for the machine work on the new rolling sensor. Mr. Steve Beck from PSI Urethane, Inc. provided valuable insights to improve the various polyurethane components in the new rolling sensor. Special thanks are extended to Dr. James Bay at Utah State University for his valuable insights on this project.

The authors would also like to thank TxDOT project director Dr. Mike Murphy, TxDOT program coordinator Mr. Ed Oshinski, and Dr. Dar-Hao Chen. Finally, the authors express appreciation to the financial support of Texas Department of Transportation.

Table of Contents

List of Figures

Chapter 1. Introduction

1.1 Background

The Rolling Dynamic Deflectometer (RDD) is a nondestructive deflection testing device that was developed by researchers at The University of Texas at Austin in the 1990s. The developmental work was funded by TxDOT research project No. 0-1422 (Bay and Stokoe, 1998). The RDD is a prototype device converted from a Vibroseis, which is a common mobile vibratory source used in geophysical explorations. Funding to purchase the Vibroseis was obtained by Professor Stokoe from the United States Air Force Office of Sponsored Research (AFOSR), the Teledyne Corporation, and the College of Engineering at The University of Texas at Austin in the mid-1980s.

A comprehensive description of the RDD is given by Bay (Bay et al., 1998). The device is a truck-mounted system that dynamically loads the pavement and simultaneously monitors the pavement response at multiple points away from the dynamic load while continuously moving at about 1 mph (1.6 km/hr). A schematic diagram of the device is shown in Figure 1.1(a). The major components include: (1) an electro-hydraulic dynamic loading system, (2) a force measurement system, (3) an array of rolling sensors that are located underneath the RDD truck, and (4) a distance measurement system. A typical rolling sensor configuration is shown in Figure 1.1(b).

The RDD has a gross weight of about 50 kips (222 kN). The hydraulic system can generate dynamic sinusoidal forces ranging from about 2 to 70 kips peak-to-peak (9 to 310 kN peak-to-peak) over a frequency range of about 20 to 100 Hz. Furthermore, the hydraulic system generates a constant hold-down force ranging from 3 to 40 kips (13 to 180 kN). During testing, the RDD applies both static and dynamic loads on the pavement surface. A typical RDD loading function is shown in Figure 1.2(a). The loading function is composed of a constant component that is the static hold-down force and a steady-state sinusoidal component that is the dynamic force. The static and dynamic forces are transferred to the pavement through two polyurethane loading rollers. The applied forces are measured by four load cells located between the loading rollers and the upper loading platform. Rolling sensors, which are located at multiple points under the RDD truck, are shown in Figure 1.1(b). The rolling sensors continuously measure the dynamic deflections due to the sinusoidal loading. Continuous deflection profiles are obtained as a result.

An example set of RDD measurements made on a flexible pavement with three rolling sensors is shown in Figure 1.2(b). Each line in Figure 1.2(b) represents a continuum of deflection readings from one rolling sensor along the test section, with the deflection values representing an averaged deflection measured over every 2 to 3 ft (0.6 to 0.9 m). In general, the deflection level decreases as the sensor is located farther away from the loading rollers. Deflection basins can also be constructed from the continuous profiles at selected locations as shown in Figure 1.2(c). The deflection basins shown in Figure 1.2(c) were measured at the three highlighted locations in Figure 1.2(b). The shape and the absolute value of each deflection basin represent the structural stiffness at different points along this flexible pavement. A photograph of the RDD performing continuous deflection testing as part of a highway project-level study is shown in Figure 1.3.

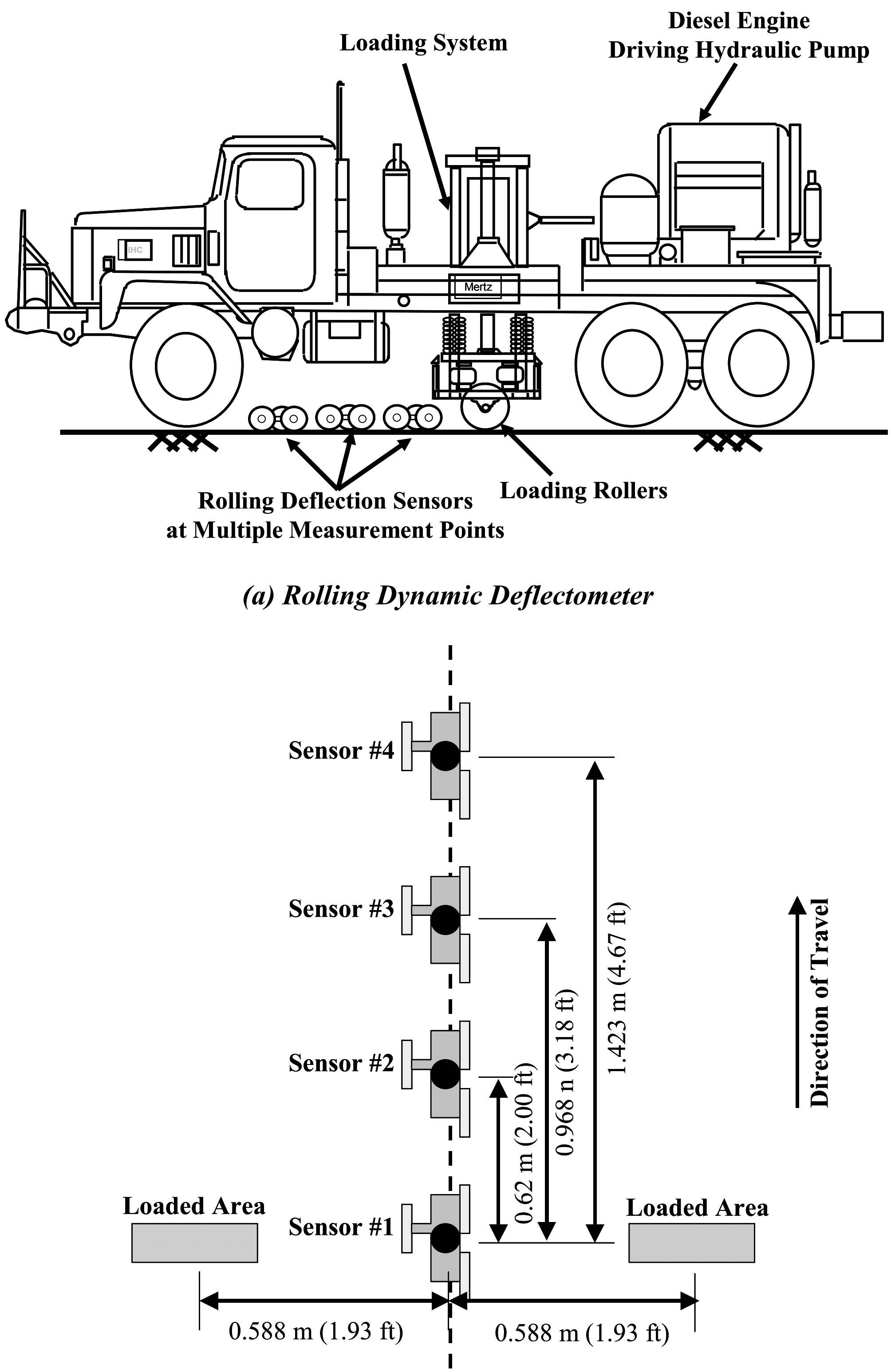

(a) Rolling Dynamic Deflectometer

(b) Typical Rolling Sensor Configuration for RDD Testing

Figure 1.1 (a) and (b). General RDD Arrangement with Rolling Sensor Array

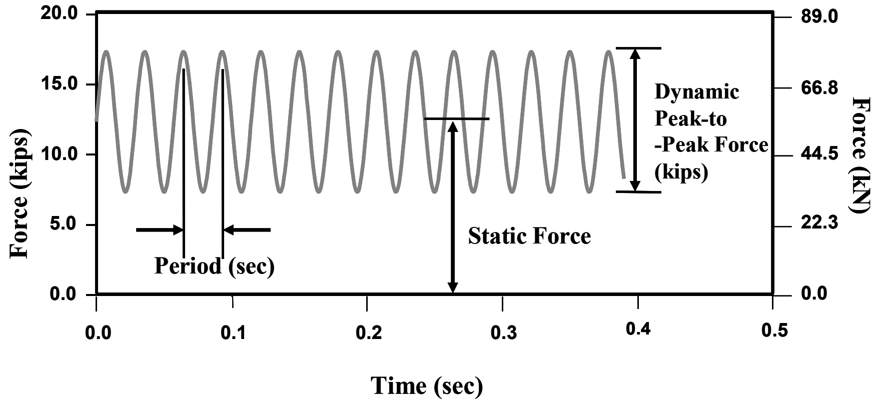

(a) Static and Dynamic Components of the RDD Loading Function

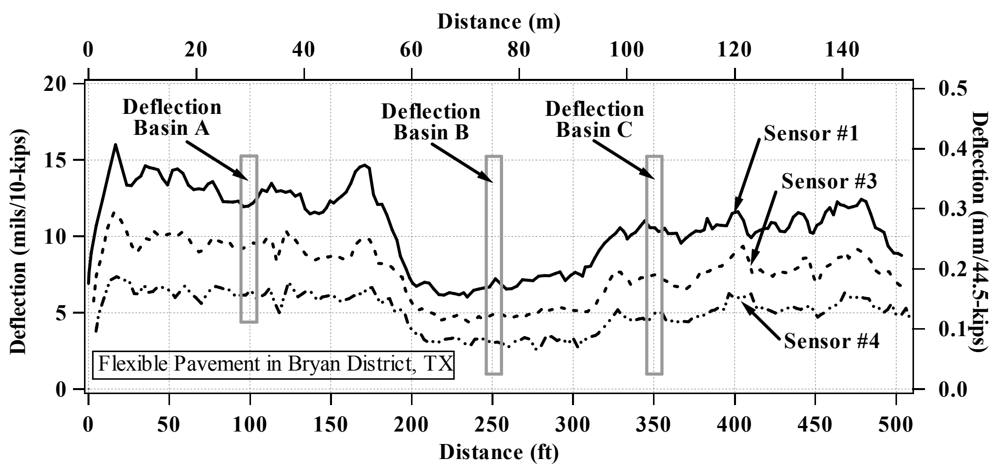

(b) Continuous Deflection Profiles at Three Different Sensor Locations Adjusted to a 10-kip (44.5-kN) Peak-to-Peak Force Level

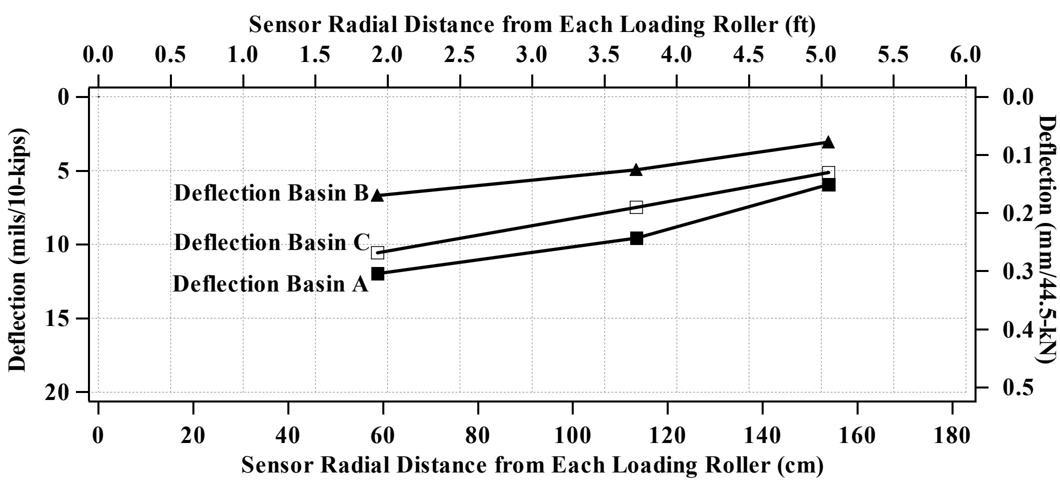

(c) Deflection Basins at Three Points along the Profile

Figure 1.2 (a), (b), and (c). Typical RDD Loading Function and Continuous Deflection Profile

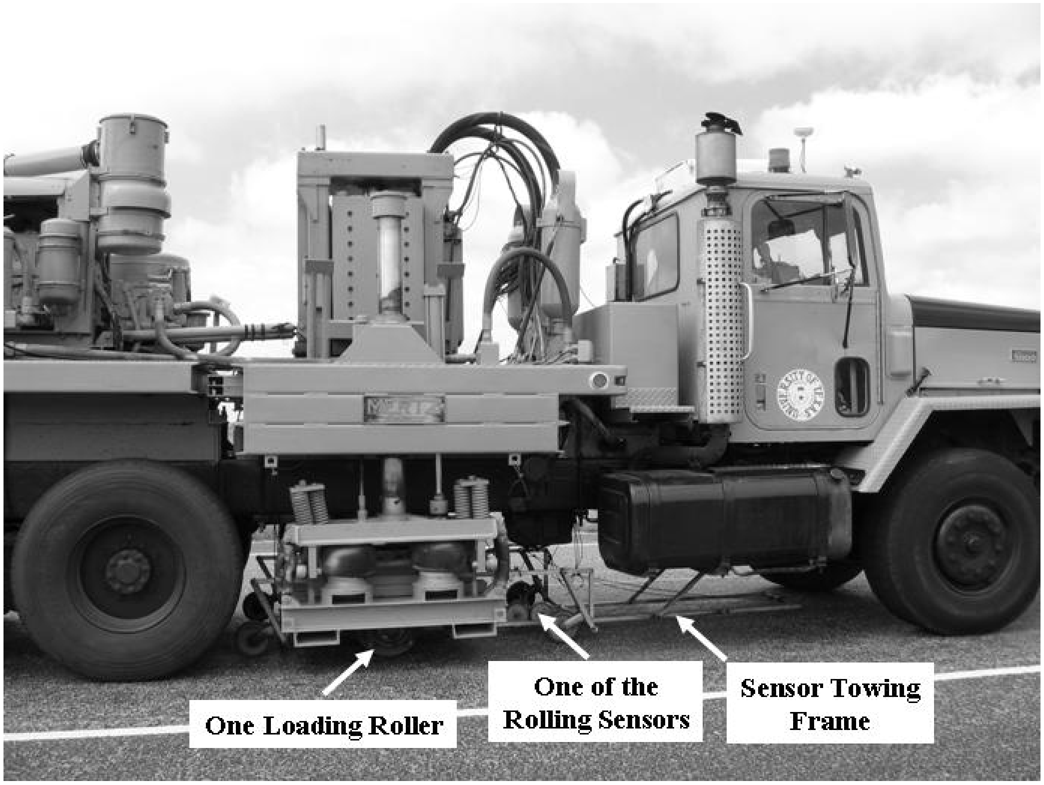

Figure 1.3 Photograph of the Rolling Dynamic Deflectometer during a Highway Project-Level Pavement Study

Over the last decade, the RDD has been used in many different project-level studies of highway and airport pavements. Compared with other nondestructive deflection testing devices, the RDD measures deflections continuously as it rolls along a pavement surface. The deflection measurements are typically presented as a continuous deflection profile, which consists of numerous individual deflection basins that are closely spaced. Pavement engineers can use the RDD deflection profile to readily identify sections with different stiffnesses along a test path. Furthermore, the confidence in the deflection measurements' capacity to detect irregularities, changes, and weak condition improves significantly as the number of samples collected per linear distance increases.

The RDD uses rolling sensors to measure pavement surface deflections at multiple locations. A rolling sensor consists of a geophone mounted on a specially designed 3-wheel cart. For the rolling sensor to provide correct measurements, it must maintain constant coupling with the pavement surface. With the current rolling sensor design, a testing speed of about 1.0 mph (1.6 km/hr) can be achieved. The primary goal of this project is to develop a new rolling sensor design that will allow the RDD to test at a higher speed. A prototype of the new rolling sensor was developed and its performance evaluated under this research project. The test speed of the RDD is expected to triple the current test speed using the newly developed rolling sensor, resulting in a nominal testing speed of 3.0 mph (4.8 km/hr).

The RDD measurement is unique in many aspects when compared to other common nondestructive deflection testing devices. First, unlike stationary devices such as the Dynaflect and Road Rater, which apply a sinusoidal force to the pavement, the raw RDD rolling sensor signal is not a pure steady-state sinusoidal signal. Instead, it is a summation of the steady-state sinusoidal signal, rolling noise, and other noise in the pavement generated by construction and vehicular activities. When the signal is presented in the frequency domain, the knowledge of the precise RDD loading frequency allows the pavement deflection signal to be separated from the rolling noise and other noise sources. Furthermore, the rolling sensor has been carefully designed and calibrated to accurately measure the deflection signal within the RDD operating frequency range.

1.2 Purpose of This Report

This report summarizes the research findings in TxDOT Research Project No. 0-4357. A new rolling sensor design is presented that triples the current RDD testing speed. The organization of this research report is as follows. In Chapter 1, a brief introduction to the RDD and objectives of the research project are presented. In Chapter 2, the design of the new rolling sensor is presented. In Chapters 3 and 4, the performance of the new rolling sensor is compared to the original rolling sensor. Both sensor designs are compared in terms of the level of rolling noise (Chapter 3) and the sensor decoupling (Chapter 4). In Chapter 5, continuous deflection profiles were collected using the new rolling sensor at different testing speeds on the TxAPT site. The new rolling sensor is shown to work well at a testing speed of 3 mph (4.8 km/hr). In Chapter 6, summary and conclusions are presented. Also, other recommendations to improve the RDD system are suggested. These improvements are necessary to implement the new rolling sensor in RDD testing, including a mechanical lifting system for the rolling sensor array.

1.3 Limitations of First-Generation Rolling Sensors

The rolling sensors are used to detect dynamic deflections of the pavement surface that are induced by the applied dynamic loading. In the initial development, a first-generation rolling sensor was developed that consisted of a 2-Hz geophone. The geophone (sensor) was mounted on a specially designed rolling cart as shown in Figure 1.4. An array of these rolling sensors was mounted under the RDD and was towed along the pavement surface during testing. Each rolling sensor was supported by three, 6-in. (152.4 mm) diameter rolling wheels. Every rolling wheel was coated with a soft polyurethane tread that is about 0.25 in. (6.35 mm) thick and 0.50 in. (12.7 mm) wide. A photograph of the first-generation rolling sensor is shown in Figure 1.5.

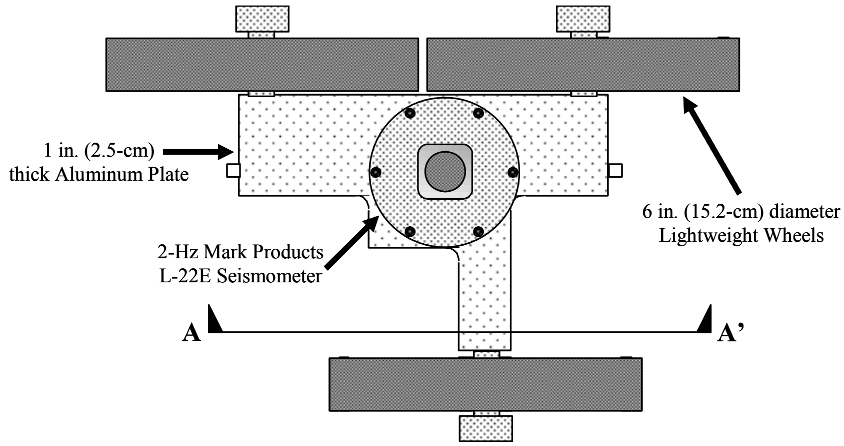

a) Plan View

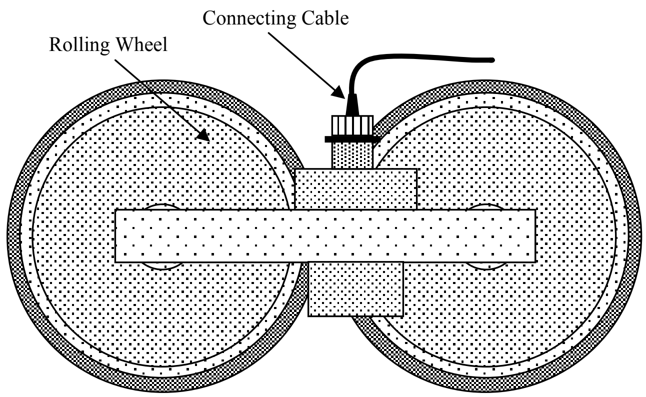

b) Cross-Sectional View (Section A-A)

Figure 1.4 (a) and (b). Schematic Drawing of the First-Generation RDD Rolling Sensor

Figure 1.5 Photograph of the First-Generation RDD Rolling Sensor

1.4 Maximum Testing Speed of First-Generation Rolling Sensors

The first-generation rolling sensor has been used in many project-level studies since the RDD was first developed. In 2004 and 2005, about 12 to 15 project-level studies were performed each year. This particular sensor design has proven to perform satisfactorily when running at testing speeds around 1.0 mph (1.6 km/hr) over a wide variety of pavement surfaces. Mathematical simulations of a rolling rigid wheel over randomly generated synthetic pavement surfaces indicate that this current sensor should not be operated at speeds over 1.4 mph (2.2 km/hr) (Bay et al., 1998). The key point in the simulation study is that it is crucial for all rolling wheels to remain in contact with the pavement surface during RDD testing for the dynamic movement of the pavement to be measured correctly.

The rolling sensor is a contact-type sensor, with the 2-Hz geophone supported on three rolling wheels. The geophone measures the dynamic movement of the pavement, and it senses the dynamic motions that are transmitted from the pavement surface through the rolling wheels to the geophone.

In the previous research study (TxDOT Research Project No. 0-1422), it was found that the negative vertical acceleration has to be limited to less than -1.0 g to prevent the rolling sensor from uncoupling from the pavement. Two major factors were identified in the report that influence the negative acceleration: (1) the rolling speed along the pavement, and (2) the diameter of the rolling wheels. Based on data collected at different project-level studies, it was found that the negative acceleration is also influenced by the road roughness. The negative acceleration due to road roughness will be higher on a rough concrete surface than a smooth asphalt concrete surface.

Since 6-in. (152-mm) diameter rolling wheels were chosen in the first-generation rolling sensor design, the only other factor that can be controlled during testing is the rolling speed. A number of assumptions were made during the previous simulation study (Bay et al., 1998). First, the rolling wheel acts as a rigid wheel. This assumption is not precisely true with the compliant polyurethane coating on each rolling wheel. Second, each rolling wheel is expected to travel through a circular arc path at constant acceleration when rolled over an obstacle. This assumption also has limitations. Because of the simplicity of the simulation, a conservative negative acceleration criterion of -0.5g was chosen. For 6-in. (152-mm) diameter rolling wheels, a rolling speed of 2 ft/sec (1.36 mph) will give a negative acceleration of less than -0.5 g. In other words, the rolling sensors should theoretically remain in contact with the pavement surface as long as the rolling speed remains at or below 1.36 mph and there are no large vertical obstacles. The relationships between rolling velocity, negative acceleration, and rolling wheel diameter are shown in Figure 1.6.

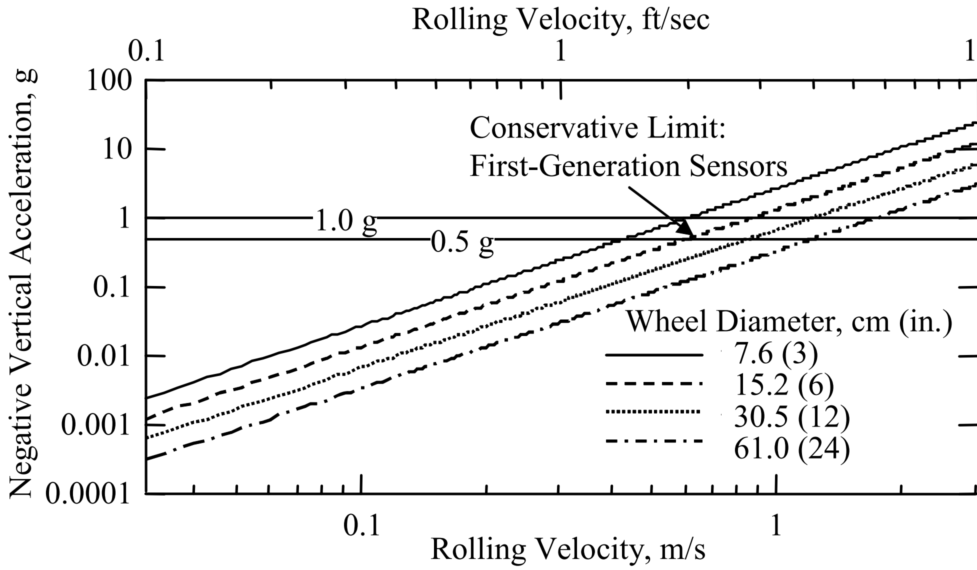

Figure 1.6 Negative Acceleration Levels Relative to Wheel Diameter and Speed along the Pavement (from Bay et al., 1998)

1.5 RDD Rolling Noise

The RDD applies a static force and a dynamic force on the pavement as was illustrated in Figure 1.2(a). The dynamic force is a single-frequency (f_o) sinusoidal load with a period $T_o=1/f_o$. In contrast, the Falling Weight Deflectometer (FWD) applies an impulsive force on the pavement by dropping different weights from pre-defined heights. Since the RDD applies a single-frequency load, it is a very robust dynamic deflection measurement technique. This robustness comes from the point that any frequencies outside the RDD loading frequency can be regarded as measurement noise, and therefore can be effectively filtered out using different digital filters. This characteristic allows the RDD to distinguish pavement surface deflections induced by the actual dynamic forcing function from other sources of noise. In most engineering applications, it is desirable to measure signals with high signal-to-noise ratios (SNR). However, this is often impossible due to different sources of noise that are present in the surrounding environment. Some of the noise sources measured during RDD testing are: (1) rolling noise caused by the rolling sensor moving along a rough pavement surface, (2) noise from motion of surrounding traffic, (3) noise from construction activities, and (4) noise from electrical power sources (i.e., 60-Hz power line noise in the United States). In fact, the signal collected by each rolling sensor during RDD testing contains a lot of noise in the time domain. Also, the noise level can be of the same order of magnitude as the deflection signal itself. A typical time record from a rolling sensor before and after it begins to roll is shown in Figure 1.7.

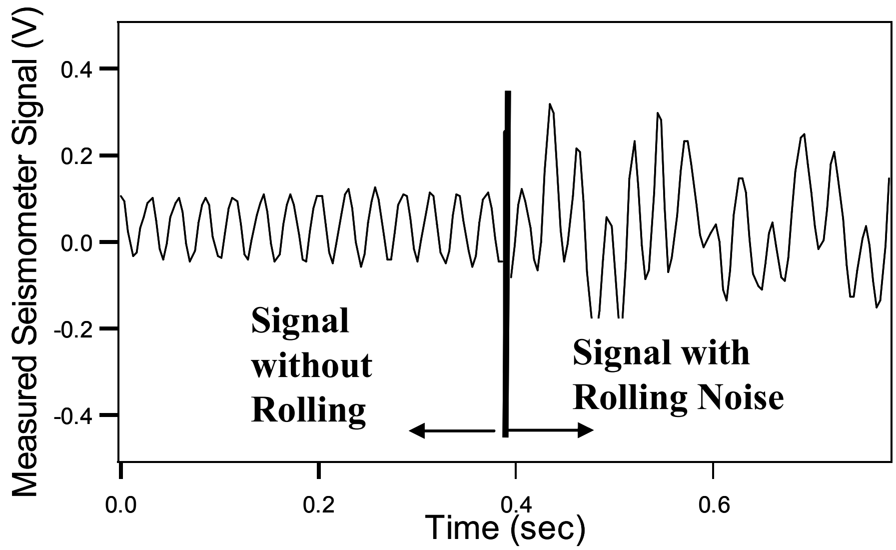

Figure 1.7 Time Record of a Rolling Sensor before and after It Starts Rolling on a Highway Pavement

After the raw RDD measurements are collected, data analysis is performed on the collected data to obtain the dynamic deflection profile along the pavement. The deflection profile is usually presented in terms of mils per 10 kips. The current data analysis procedure uses a notch-pass digital filter that attenuates noise signals at frequencies outside the RDD operating frequency. As a result, only deflections at the RDD operating frequency are identified and used to calculate the continuous deflection profile. This data analysis procedure requires the knowledge of the precise RDD operating frequency. This knowledge is available because it is the frequency of the dynamic loading delivered to the loading rollers.

Even though RDD testing can attenuate noise effectively, it is always good practice to reduce the level of noise in the measurements. Since the typical RDD operating frequency ranges from 20 to 45 Hz, the 60-Hz power line noise is easily filtered out and does not affect the measurements in any significant way. However, both the surrounding traffic noise and rolling noise have wide-band frequencies, and the characteristics of their spectra may affect the RDD measurements if much energy is concentrated near the selected RDD operating frequency. In this case, the digital filters would be more difficult to use to separate noise from the actual RDD deflection signal. Figure 1.8(a) is a three second time record of a typical RDD rolling sensor measurement, and Figure 1.8(b) is the same signal represented in the frequency domain. It is difficult to judge the quality of the measurement by just looking at the RDD rolling sensor signal in the time domain. But the RDD signal at 35 Hz is clearly shown in the frequency domain. All the other frequency components shown in Figure 1.8(b) are regarded as noise. As can be seen in Figure 1.8(b), there is obviously some noise at the RDD operating frequency, but it is very small percentage (typically less than a few percent) of the RDD deflection signal.

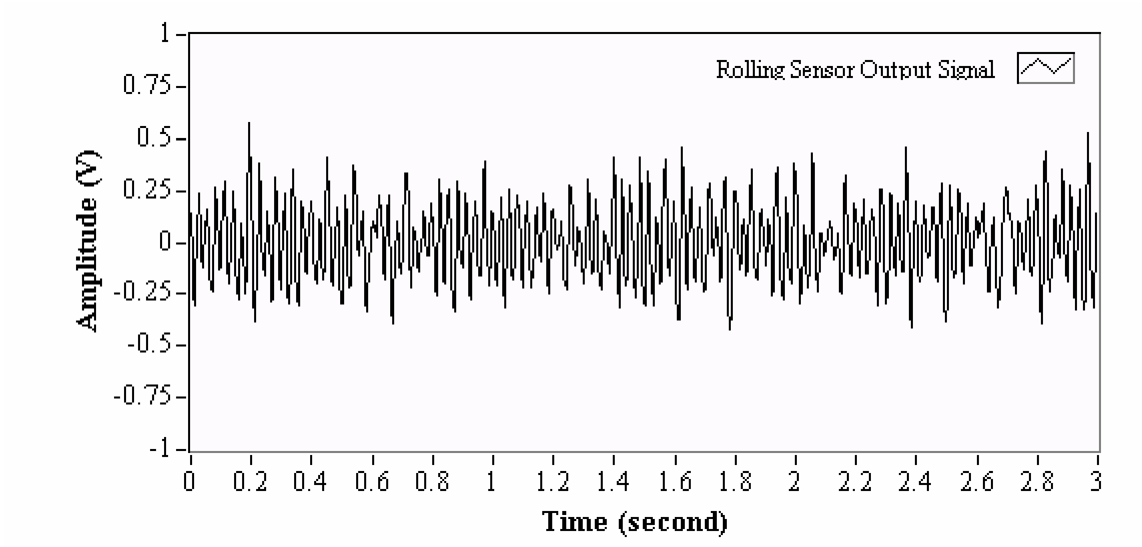

(a) Time Domain

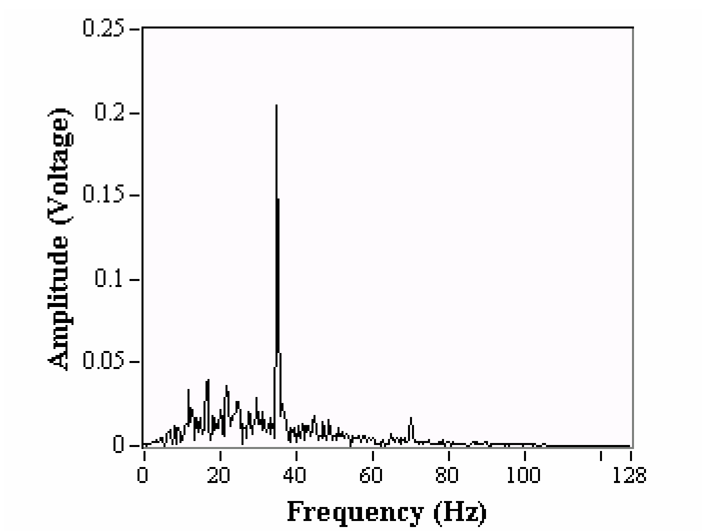

(b) Frequency Domain

Figure 1.8 (a) and (b). Typical RDD Rolling Sensor Output Signal in the Time and Frequency Domains

Rolling noise spectra calculated using a 6-inch (152 mm) diameter wheel rolling on a synthetic pavement are shown in Figure 1.9. Different diameters of rolling wheels will theoretically generate different noise spectra when rolled at a speed of 1 ft/sec (0.68 mph). As the rolling wheel diameter increases, the level of rolling noise tends to decrease as shown in Figure 1.9.

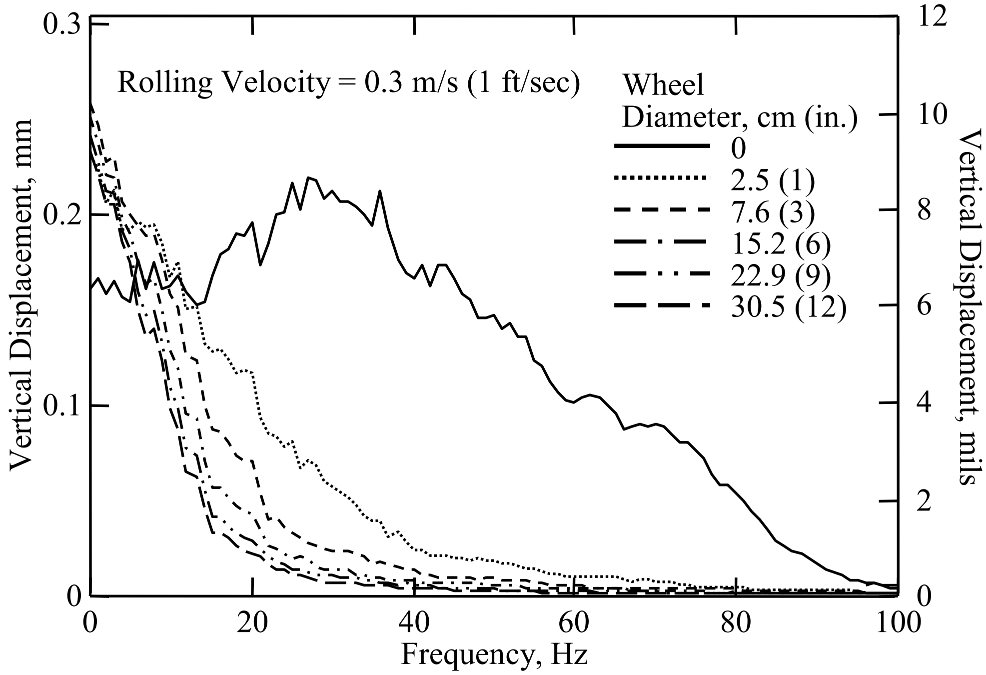

Figure 1.9 Vertical Displacement Spectra for Wheels with Various Diameters Rolling over a Synthesized Pavement Surface (from Bay et al., 1998)

To reduce the level of rolling noise in the RDD measurement, compliant wheels, which are metal wheels coated with polyurethane, were chosen instead of rigid metal wheels with no coating. One of the short-comings for using a compliant wheel is that the polyurethane coating acts as a compressible spring, and therefore introduces a resonance to the rolling sensor. However, this problem is resolved by carefully designing the rolling sensor such that the resonant frequency is located outside the frequency that is of interest in RDD measurements. The calibration curves for the first-generation rolling sensors are shown in Figure 1.10. As seen in the figure, the resonant frequency is slightly above 100 Hz.

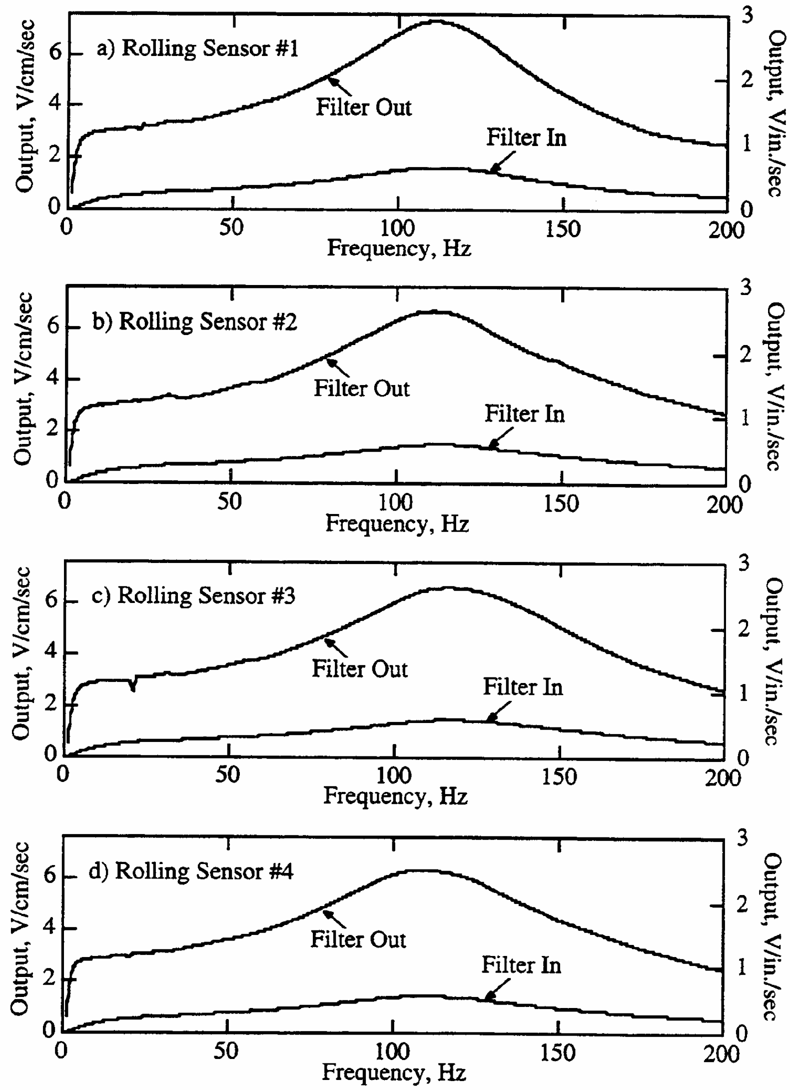

Figure 1.10 Calibration Curve of the First-Generation Rolling Sensor (from Bay et al., 1998)

1.6 Summary

The Rolling Dynamic Deflectometer is a nondestructive deflection testing device that is used in project-level studies to assist in the evaluations of highway and airport pavements. The RDD was developed by researchers at UT in the 1990s. At present time, the testing speed of the RDD is about 1 mph (1.6 km/hr). The testing speed is limited by the rolling sensors. The limiting speed is controlled by the size of the wheels (6 in./152 mm in diameter) of the rolling sensors as discussed in this chapter. If testing is performed at speeds greater than 1 mph (1.6 km/hr), the rolling sensors can decouple from the pavement and, hence, invalidate the measurements. The sensor decoupling issue can theoretically be eliminated if the rolling sensor is replaced by a non-contact transducer (e.g., displacement laser sensors). However, a non-contact transducer has its own measurement noise and equipment-compatibility considerations which can limit its usefulness in the RDD set-up. Based on the experience reported by ERES Consultants in a Rolling Wheel Deflectometer (RWD) pilot test study (ERES, 2004), it is often difficult to maintain an accurate reference datum for the displacement laser. Pavement features such as bridge joints, culverts and patching in the road surface often cause excessive bouncing of the RWD trailer, resulting in erroneous spikes in the deflection profile. The RDD environment with all pieces of equipment vibrating at various levels is a more harsh environment than the RWD set-up and obtaining an accurate reference datum is even more challenging.

With this background, the design and testing of a second-generation rolling sensor was undertaken. The key design considerations were: (1) larger wheels on the rolling sensor carriage, and (2) the addition of a hold-down force to help prevent decoupling from the pavement at higher testing speeds. These points are addressed in Chapter 2.

Chapter 2. Design and Construction of the Second-Generation Rolling Sensor

2.1 Development of the Second-Generation Rolling Sensor

The primary objective of this research project is to increase the RDD testing speed from 1 to 3 mph (1.6 to 4.8 km/hr). The only technical hurdle in accomplishing this objective is developing rolling sensors which perform properly at 3 mph (4.8 km/hr). The two major factors that limit the existing testing speed are: (1) the negative acceleration of the rolling sensor as it moves along a rough surface, and (2) the level of rolling noise measured during testing. To accomplish the objective of increasing the testing speed, new rolling sensors were designed . These new sensors are designed so that the RDD testing speed can be increased by a factor of three. The new rolling-sensor design is called the second-generation rolling sensors hereafter.

During the duration of the project, two rolling sensor designs evolved. The first design provides an additional hold-down force by adding a mass suspended on a soft spring, and the second design provides an additional hold-down force by pressurizing a massless air spring, which is located at the top of each rolling sensor. In the end, the second-generation rolling sensors were built using the second design, which uses air spring for an additional hold-down force. This design was preferred because it allows a larger hold-down force to be applied and the geophone is located lower in the rolling sensor assembly. Four rolling sensors were constructed using the second design. In this chapter, the design, fabrication, and laboratory calibration procedures of the second-generation rolling sensors are discussed.

2.1.1 Negative Vertical Acceleration - Maintaining Coupling with Pavement

A critical factor for successful RDD measurements is the maintenance of good coupling between the pavement surface and the rolling sensors. This coupling is necessary because the rolling sensors need to be able to sense the motion of the pavement that is induced by the RDD loading system. By limiting the negative vertical acceleration of the rolling sensors to less than –0.5g, it can be assured that the rolling sensor stays coupled with the pavement surface during RDD testing. Two major factors that control the negative vertical acceleration were identified in the previous TxDOT research project 0-1422. These factors were: (1) the rolling speed and (2) the diameter of the rolling wheels.

Two improvements to the existing rolling sensor design were made to increase rolling speed. First, an additional hold-down force was provided to each rolling sensor. The allowable negative vertical acceleration is increased by the addition of a hold-down force on each sensor. Second, the diameter of the rolling wheels was also increased. Larger-diameter rolling wheels will result in a smaller negative vertical acceleration than smaller-diameter rolling wheels at the same rolling speed.

2.1.2 Rolling Noise

At the current stage of RDD development, contact-type sensors are used to measure dynamic pavement deflection. The dynamic pavement deflection induced by the RDD dynamic force is measured by the geophone mounted on each rolling sensor. As long as a contact-type sensor is used, rolling noise will always be present in these measurements. Since the rolling noise has a detrimental effect on the deflection measurements, this factor has always been a major consideration in the rolling sensor design. Hence, the second-generation rolling sensors have larger diameter rolling wheels to reduce the level of rolling noise.

Signals collected with the rolling sensors contain noise, and the noise can be of the same order of magnitude in the time domain as the signal that represents the dynamic pavement response. This fact has been discussed in Chapter 1 and was illustrated in Figures 1.7 and 1.8. Appropriate signal processing techniques are used to attenuate noise. The noise can usually be filtered out because the loading system of the RDD loads the pavement at a single operating frequency, f_o. However, digital filters can only be used to attenuate rolling noise at frequencies other than the chosen operating frequency. They cannot distinguish the rolling noise component that is at the operating frequency from the RDD signal. Therefore, it is very beneficial to minimize rolling noise in the RDD operating frequency range.

Even though the RDD data processing techniques can effectively attenuate most of the noise that is away from the chosen operating frequency, it is still important to minimize the rolling noise for two reasons. First, reduction of rolling noise will increase the Signal-to-Noise Ratio (SNR) of the measurements. This is important because digital filters cannot distinguish between noise and signal if both of them occur at the operating frequency. Second, most digital filters will have increasing difficulty in resolving the frequency components that are closely located. In this case, the signal needs to be resolved at the operating frequency. The second point is related to the relationship between bandwidth in the pass-band of the filter and the attenuation level at the stop-band of digital filters.

2.2 Design Considerations for Rolling Sensors

2.2.1 Overview

The design of the rolling sensor affects the testing speed, accuracy of the deflection measurements, and the measured rolling noise spectra. Therefore, the rolling sensor design is essential to the overall performance of the RDD. Three major factors that govern the design of the second-generation rolling sensors are: (1) the frequency response of the rolling sensors, (2) the hold-down force required to maintain good coupling of the rolling sensors at the target testing speed, and (3) the acceptable level of rolling noise. It is important to note that all three factors are closely related.

2.2.2 Frequency Response of a Rolling Sensor

The frequency response of a rolling sensor can be measured by taking the ratio between the rolling sensor motions and the pavement motions at different frequencies. The frequency response illustrates the dynamic characteristics of the system. The rolling sensor can be modeled as a single-degree-of-freedom (SDOF) system with a lumped mass (m) supported by a spring that has a spring constant (k) and a viscous dashpot coefficient (c). Such a SDOF system is shown in Figure 2.1.

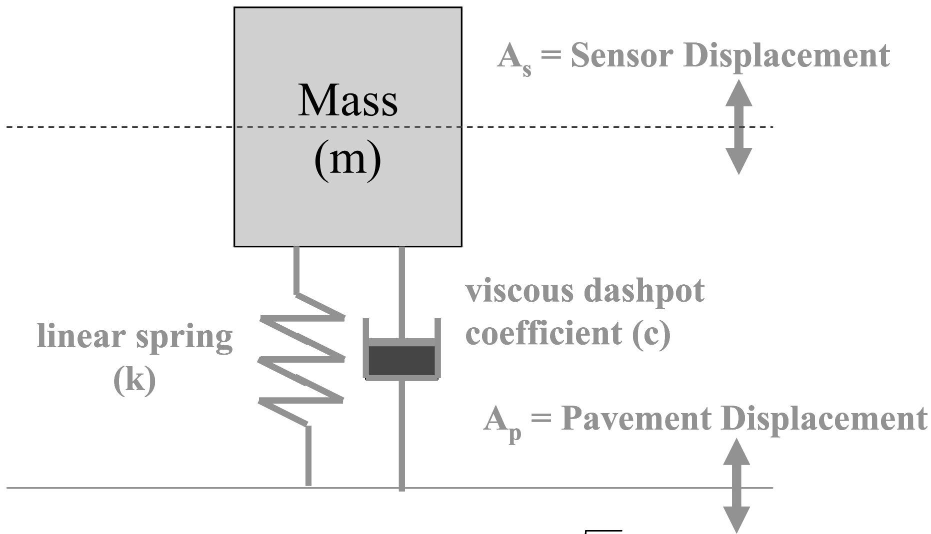

$$\omega_R = \text{resonant circular frequency} = \sqrt{\frac{k}{m}}$$

$$\omega_D = \text{damped circular frequency} = \omega_R\sqrt{1-D^2}$$

$$c_{cr} = \text{critical viscous damping coefficient} = 2m\omega_R$$

$$D = \text{damping ratio} = {}^{c}\!/_{2m\omega_R} = {}^{c}\!/_{c_{cr}}$$

Figure 2.1 Single-Degree-of-Freedom (SDOF) System Used to Model a Rolling Sensor

The RDD loading system can operate between frequencies of 5 and 100 Hz. However, RDD testing is typically performed between frequencies of 30 and 45 Hz. For all practical purposes, it is desirable to have a constant frequency response over the range of frequencies used in RDD testing. Furthermore, the resonant frequency (ω_r) of a rolling sensor should be far away from the RDD operating frequency range. In fact, the resonant frequency (ω_r) should be well above the operating frequency so that lower frequencies (often below 20 Hz) associated with traffic do not resonate the rolling sensor. There are three main ways to achieve a high-resonant-frequency SDOF system. Two of these ways are: (1) a lighter rolling sensor (i.e., decrease the mass of the SDOF system) increases the ω_r, (2) increasing the stiffness of the rolling sensor (i.e., increase the spring constant (k) of the SDOF system) also increases the ω_r. Since the polyurethane thread on the rolling wheels and the top air spring are the only deformable parts in the rolling sensor, the stiffness of this SDOF system is mainly controlled by the stiffness property of the polyurethane components. The third way to achieve a high-resonant-frequency SDOF system is to increase the hold-down force, which will increase the stiffness of the overall system and consequently also increase the ω_r.

2.3 Second-Generation Rolling Sensor—First Design

During this project, two rolling sensor designs were considered. Both designs involved some type of system to provide an additional hold-down force. The main difference between the two designs is the way the hold-down force is provided to the rolling sensor. The first design involved a heavy mass supported on a soft spring as shown in Figures 2.2 and 2.3. This hold-down system is enclosed inside a cylindrical acrylic tube, and the acrylic tube forms part of the rolling cart.

Three, 12-in. (305-mm) diameter aluminum wheels support this rolling sensor. In addition, this rolling sensor design has hinge connections at both ends of the cart where the positioning mechanisms are located. The positioning mechanisms are used to position the rolling sensor within the towing frame (see Figure 1.3). The hinge connection minimizes noise transmission from the RDD truck through the towing frame to the rolling sensor as well as minimizing noise transmission by the towing frame itself.

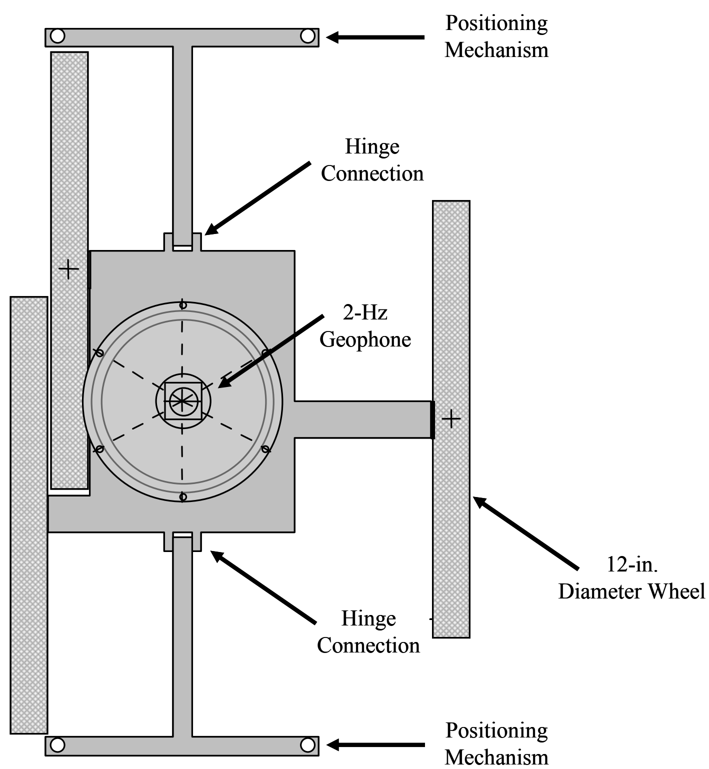

Figure 2.2 Top View of the First Design Considered for the Second-Generation Rolling Sensor

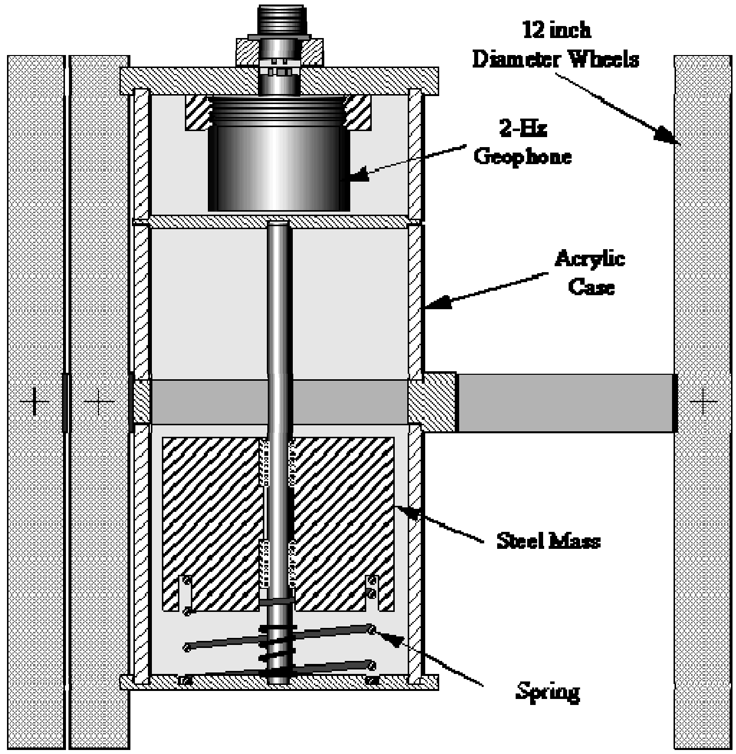

Figure 2.3 Side View of the First Design Considered for the Second-Generation Rolling Sensor

There are major limitations to this rolling sensor design. First, the amount of hold-down force is controlled by the size of the steel mass. The size of the steel mass is in turn limited by the size of each rolling sensor. It is important not to make a rolling sensor with large footprint, which will cause the measurement to be averaged over a large area. Second, there must be sufficient headroom provided for the steel mass to move as the rolling sensor rolls along the pavement. It is detrimental if the steel mass ever reaches the top, because this would affect the reading of the geophone and might even uplift the rolling sensor in the worst case. Due to the limited hold-down force and the head-room restrictions, this first rolling sensor design was abandoned. There are a number of reasons to abandon this first rolling sensor design. They are: (1) the magnitude of the hold-down force is limited by the physical size of the rolling sensor, (2) insufficient space exists underneath the RDD truck to allow free traveling of the steel mass, and (3) the geophone is located relatively far above the pavement surface.

2.4 Second-Generation Rolling Sensor—Second Design

The second-generation rolling sensors were built using the second design. The rolling carriages and rolling wheels are made at the machine shop of the Physical Plant Department, The University of Texas at Austin. The entire rolling carriage is built from aluminum alloy. When compared with the first-generation rolling sensor, the size of the carriage is substantially increased to accommodate the externally applied hold-down force and the larger rolling wheels. Each sensor is equipped with either 9-in. (229-mm) or 12-in.

(305-mm) diameter rolling wheels for rolling noise reduction. Furthermore, this wheel arrangement minimizes the footprint of the rolling sensor.

The second rolling sensor design uses a pressurized air spring to provide the required hold-down force. A custom-made polyurethane air spring is attached to the top of each rolling sensor, and a significant hold-down force can be achieved even when the air spring is pressurized at a small pressure. For example, the air springs can each be pressurized individually from 1 to 5 psi (6.9 to 34.5 kPa), resulting in around 7 to 35 lb (31 to 156 N) of hold-down force, respectively. The second rolling sensor design is shown in Figures 2.4 through 2.8.

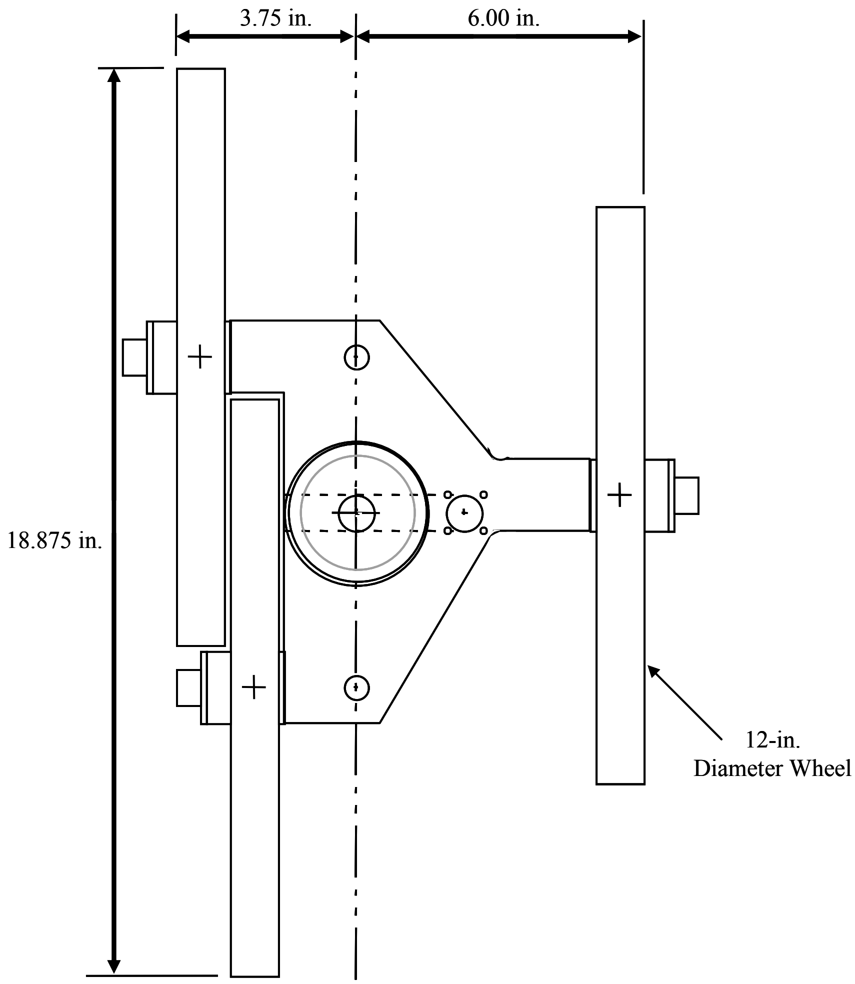

Figure 2.4 Plan View of the Second Design Considered for the Second-Generation Rolling Sensor

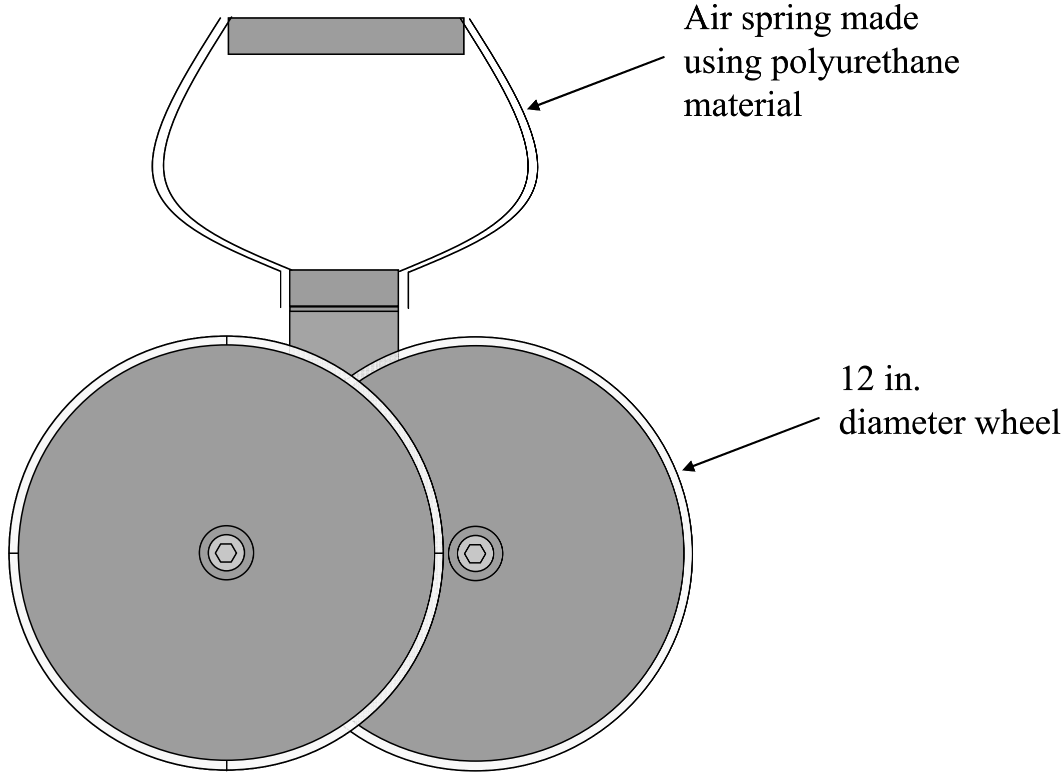

Figure 2.5 Side View of the Second Design Considered for the Second-Generation Rolling Sensor

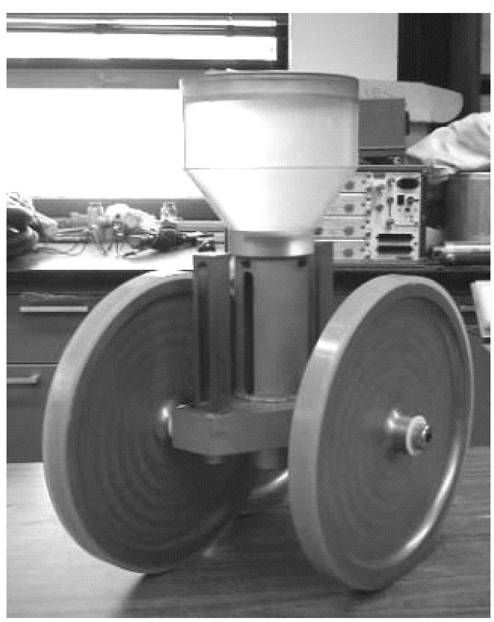

Figure 2.6 Photograph of the Second Design Considered for the Second-Generation Rolling Sensor

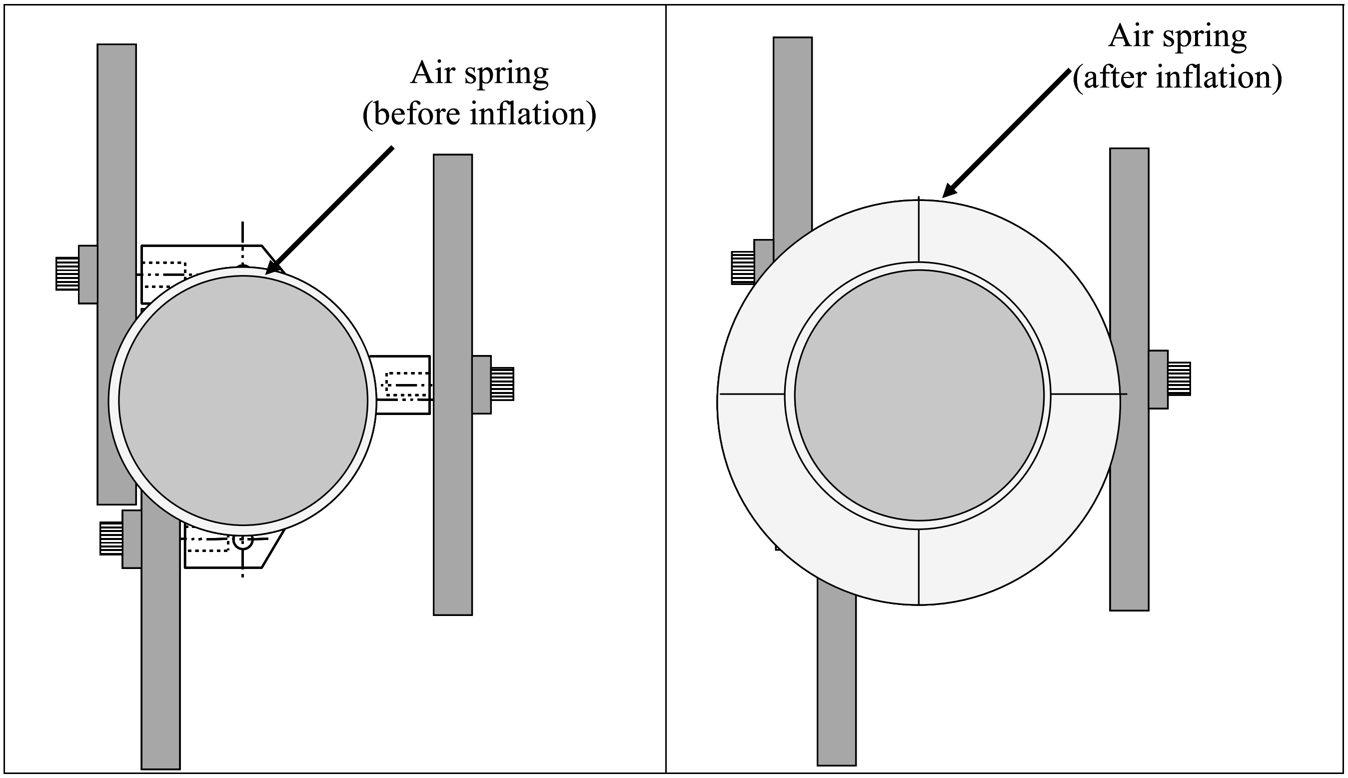

Figure 2.7 Top View of the Air Spring Used in the Second-Generation Rolling Sensor

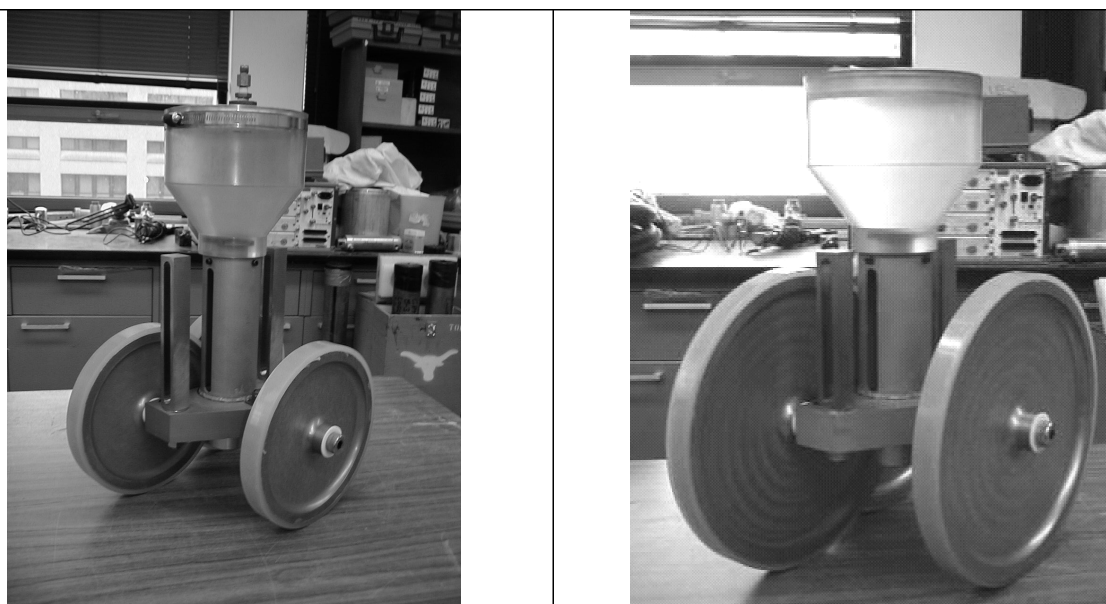

(a) 9-in. diameter rolling sensor

(b) 12-in. diameter rolling sensor

Figure 2.8 Photographs of the Second-Generation Rolling Sensors

This second-generation rolling sensor design has two components that are made of polyurethane material. These components include the air spring and the coating on the rolling wheels. All of these components are custom molded by PSI Urethanes, Inc. located in Austin, Texas. There are many reasons for choosing polyurethane. Some of the reasons are as follows:

(1) high abrasion and impact resistances,
(2) good bonding properties with metals,
(3) high chemical resistance,
(4) a wide range of hardnesses, and
(5) more durability than most conventional elastomers and plastics.

Typical hardness levels and applications are shown in Figure 2.9.

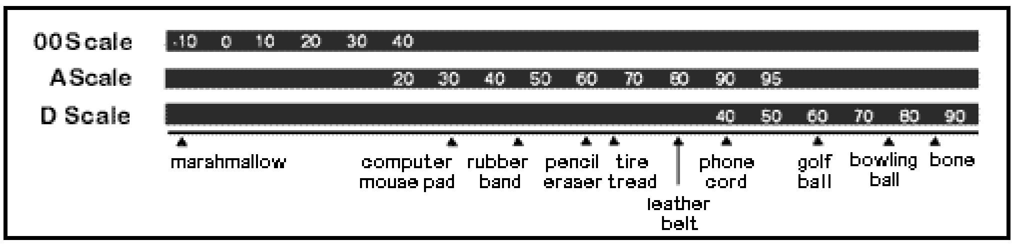

Figure 2.9 Typical Hardness Range for Polyurethane and Their Applications (from PSI Urethanes, Inc. brochures, Austin, Texas)

Each air spring is made from polyurethane with a 40 durometer on the A scale as shown in Figure 2.9. An aluminum mold was used to cast the air spring. This aluminum mold was made at the machine shop in the UT Austin Department of Civil Engineering and then used by PSI Urethane, Inc. to cast the polyurethane air spring. This soft polyurethane was chosen because it can minimize vibrations between the towing frame and the rolling sensor. Also, the polyurethane air spring is nearly massless. As shown in Figure 2.9, the 40 durometer on the A scale is approximately equivalent to the hardness of rubber bands. The shape of the air spring was specially designed so that it will approach a sphere when pressurized. This is important because the geometry of a sphere should minimize the chance of over-turning the rolling sensors. Each air spring has a bottom cross-sectional area of 7 in^2, and if pressurized at 5 psi (34.5 kPa), an equivalent hold-down force of 35 lb (16 kg) is provided to each rolling sensor. A photograph of the configuration used to connect the second-generation rolling sensors to the towing frame is shown in Figure 2.10.

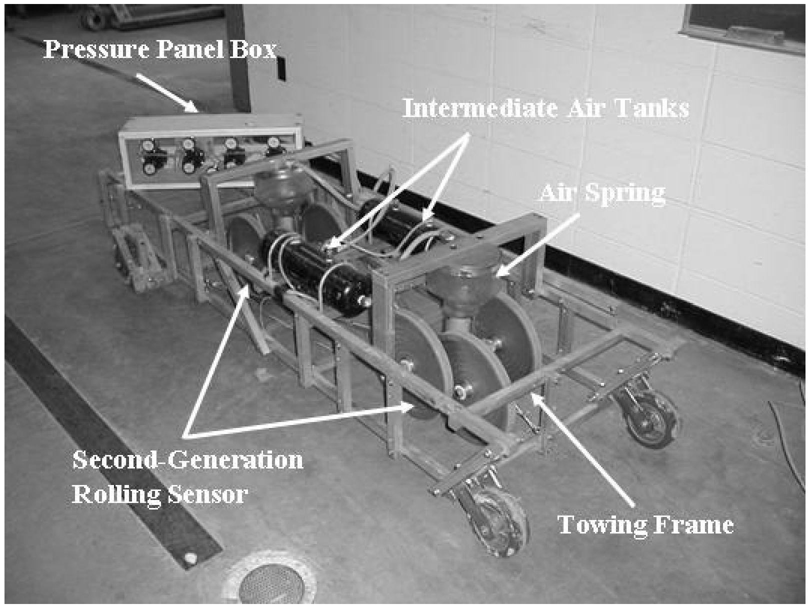

Figure 2.10 Photograph of Towing Frame and Second-Generation Rolling Sensors

In this rolling sensor design, special considerations have been made to minimize the level of rolling noise. First, the diameter of rolling wheels was increased. The diameter of the rolling wheels was increased from 6 in. (152 mm) to 9 in. (229 mm) in some sensors and to 12 in. (305 mm) in other sensors. Sensor #1 was constructed with 9-in. (229-mm) diameter rolling wheels, and Sensor #2, #3 and #4 were constructed with 12-in. (305-mm) diameter rolling wheels. The use of 9-in. (229-mm) diameter rolling wheels was necessary for Sensor #1 because of limited space underneath the RDD truck in the location of Sensor #1. These smaller diameter wheels were positioned at locations that were closer to the loading rollers because the Signal-to-Noise Ratio (SNR) at these locations tends to be higher. The 12-in. (305-mm) diameter rolling wheels will be used to improve the SNR at locations that are farther away from the loading rollers.

Second, each rolling wheel is coated with a stiff polyurethanes coating of 0.25 in. (6.4 mm) in thickness. This coating serves to protect the aluminum hub and to reduce the noise level during rolling. There is a trade-off between the resonant frequency and the level of rolling noise. Intuitively, a softer polyurethane thread should reduce the level of rolling noise. However, a softer polyurethane thread has a lower spring constant (k) that results in a lower resonant frequency for the rolling sensors. Therefore, a tradeoff is needed between the level of rolling noise and the overall frequency response of the rolling sensor system. A polyurethane material with a hardness of 50 durometer on the D scale was chosen. This material is roughly equivalent to the hardness between a phone cord and a golf ball as seen in Figure 2.9.

Aluminum molds for the rolling wheel coatings were made at the machine shop in the Physical Plant Department at The University of Texas at Austin. The dimension of the aluminum mold has to be very precise so that each rolling wheel has a uniform polyurethane coating. This is crucial because a non-uniform polyurethane coating would change the stiffness of the rolling sensor during testing and would also introduce unnecessary noise due to uneven rotation of the rolling wheels. The polyurethane coating was molded by PSI Urethane, Inc. There are two main reasons for using hard polyurethane material as a coating for the rolling wheels. First, since the stiffness of each rolling sensor is controlled by properties of the rolling-wheel coating, a SDOF system with a higher stiffness (k) will have a higher resonant frequency. A high resonant frequency is desirable in the rolling sensor design as discussed earlier. Second, a stronger bonding between the polyurethane coating and the aluminum hub can avoid damaging the rolling wheels during testing. However, the use of a stronger polyurethane coating is expected to have a small negative effect on the level of rolling noise.

2.5 Rolling Sensor Modeled as a Single-Degree-Of-Freedom (SDOF) System

During RDD testing, the rolling sensor is used to measure the dynamic part of the pavement deflection induced by the two RDD loading rollers. A rolling sensor is basically a geophone mounted on a specially designed rolling cart. For the rolling sensor to accurately measure the pavement deflection, the rolling sensor has to stay coupled with the pavement surface at all times. The motion of the rolling sensor can be simply modeled as a single-degree-of-freedom (SDOF) system, which consists of a lumped mass, m, attached to a linear spring with a spring constant, k, and a viscous damper with a viscous damping coefficient, c. A SDOF model and associated parameters are illustrated in Figure 2.1.

When the rolling sensors move along a pavement surface, the deflection of the pavement, A_p, is transmitted through the rolling sensor. Then the geophone measures the displacement of the rolling sensor, A_s. The mathematical solutions which describe motion of the rolling sensor when it is subjected to a pavement excitation can be represented by Equations 2.1 and 2.2 (Richart et al., 1970). The graphical representation of Equations 2.1 and 2.2 is shown in Figure 2.11.

$$\frac{A_S}{A_P} = \frac{\sqrt{1+\left(2D\frac{\omega}{\omega_r}\right)^2}}{\sqrt{\left[1-\left(\frac{\omega}{\omega_r}\right)^2\right]^2+\left[2D\frac{\omega}{\omega_r}\right]^2}} \tag{2.1}$$

$$\tan\phi_1 = \frac{2D\left(\frac{\omega}{\omega_r}\right)}{1-\left(\frac{\omega}{\omega_r}\right)^2\left(1-4D^2\right)} \tag{2.2}$$

where

A_s	= peak amplitude of rolling sensor displacement
A_P	= peak amplitude of ground excitation
ϕ_1	= phase angle between the rolling sensor motion relative to the motion of the pavement surface
c	= viscous damping coefficient
c_{cr}	= critical viscous damping coefficient
D	= damping ratio = c / c_{cr}
ω	= angular frequency
ω_r	= angular resonant frequency

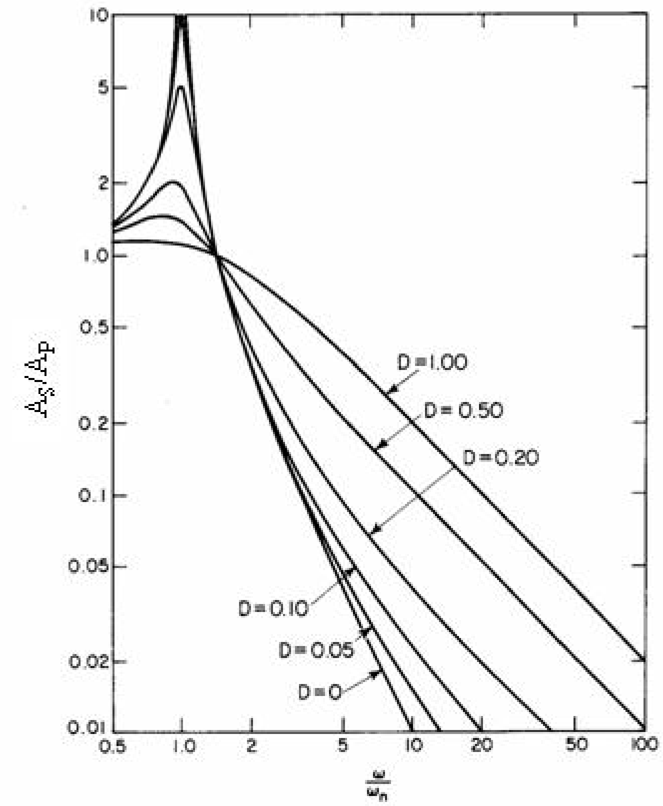

(a) Frequency Response

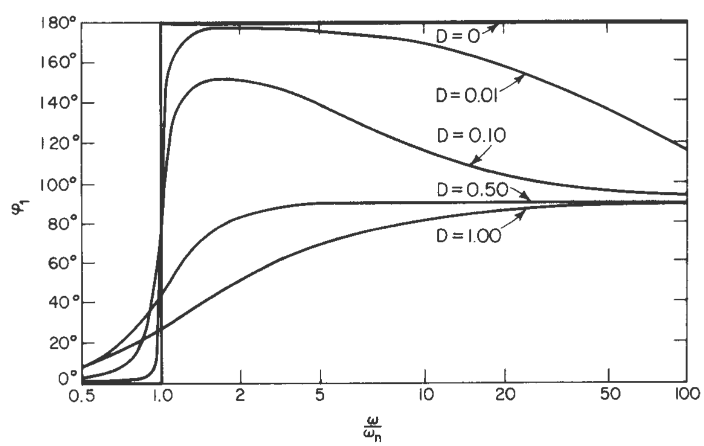

(b) Phase Response

Figure 2.11 (a) and (b). Graphical Representation of the Dynamic Motion of a Rolling Sensor from Movement of the Pavement (after Richart et al., 1970)

2.6 Laboratory Calibration of the Rolling Sensors

Each rolling sensor needs to be calibrated individually in the laboratory before it can be used to make deflection measurements in the field. The layout of the equipment used for laboratory calibration of the second-generation rolling sensors is shown in Figure 2.12. Photographs of the laboratory calibration setup are shown in Figures 2.13 and 2.14. Each rolling sensor was calibrated with the air-spring pressurized to 5 psi. Furthermore, the reaction frame which provides the reaction force against the pressurized air-spring, was rigidly bolted to the shaker. A heavy reaction frame was not needed because the connecting rods were in tension when the air-spring was pressurized, providing the required hold-down force for the sensor.

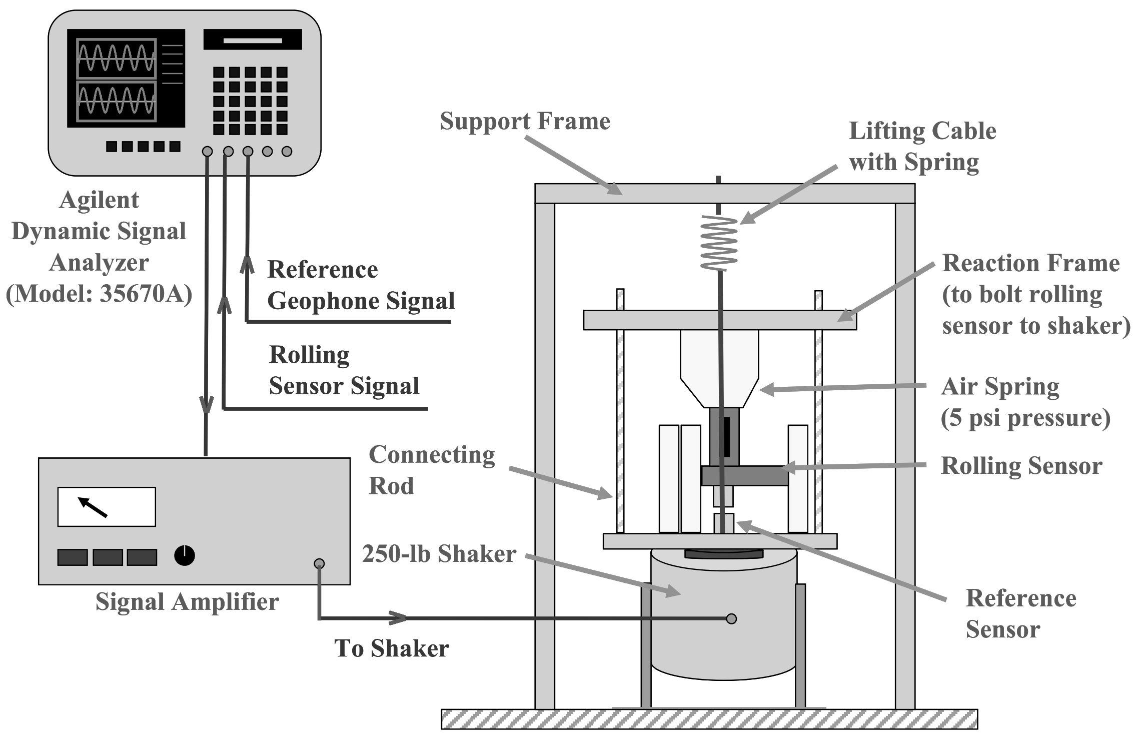

Figure 2.12 Schematic Illustration of the Laboratory Calibration Setup of a Second-Generation Rolling Sensor

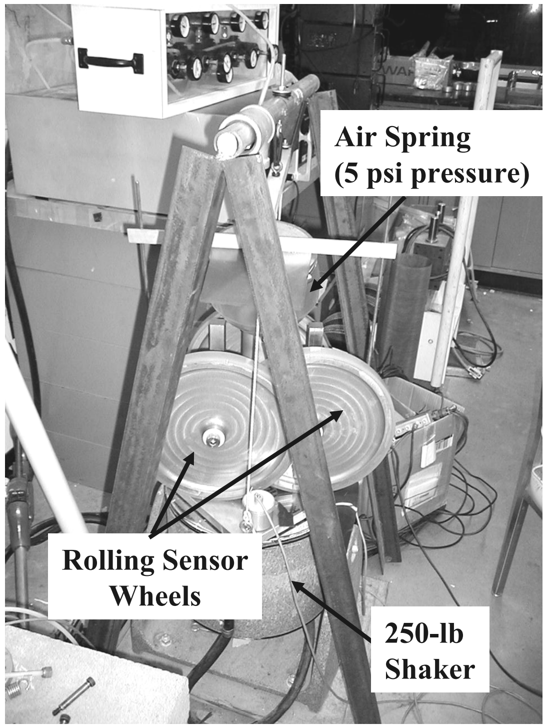

Figure 2.13 Photograph of the Laboratory Calibration Setup of a Second-Generation Rolling Sensor

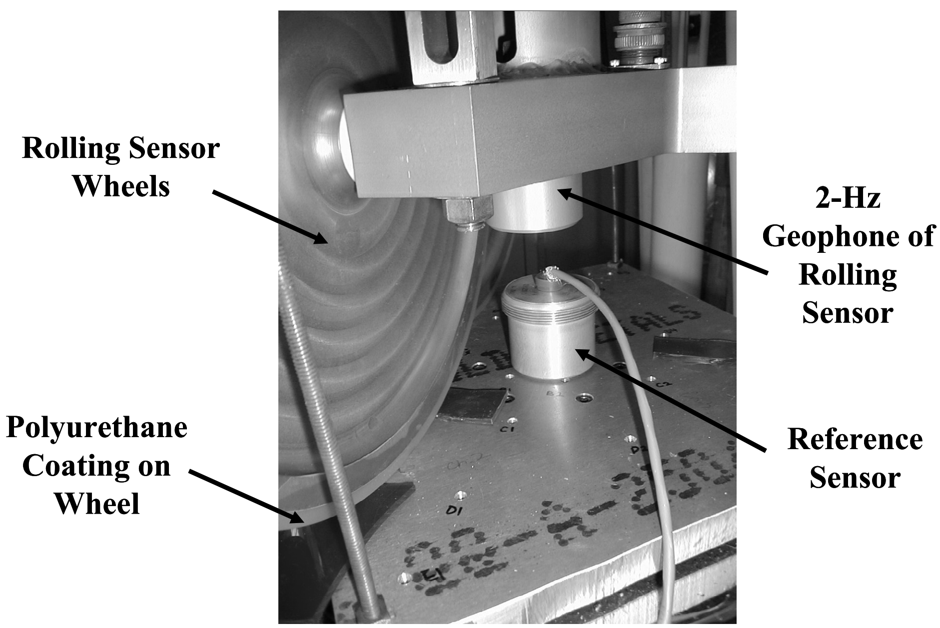

Figure 2.14 Photograph of the Reference Geophone Sensor Used in the Laboratory Calibration Setup Procedure

The laboratory calibration procedure involves placing a rolling sensor on a shake table and monitoring the voltage output of the geophone inside the rolling sensor over a wide range of known shaking levels. The voltage output is a function of the amplitude and driving frequency of the shake table. An Agilent dynamic signal analyzer (Model: 35670A) is used to control and monitor the frequency response of the whole calibration procedure. A swept sine is set to run from 5 to 200 Hz. This frequency range is sufficient to cover the entire frequency range that is of interest to RDD testing. First, the signal analyzer passes the frequency sweep signal to the signal amplifier. The signal is then amplified by the signal amplifier, and it is used to drive the 250-lb (113-kg) electromagnetic shaker.

The rolling sensor rests on a 0.75-in. (19-mm) thick aluminum plate that is bolted to the central moving core of the electromagnetic shaker. The assumption that the aluminum plate remains rigid during the calibration procedure is made. This assumption means that each rolling wheel has the same excitation motion. The calibration curve of a second-generation rolling sensor with 12-in. diameter rolling wheel and an air spring that was pressurized to 5 psi (34.5 kPa) is shown in Figure 2.15. The calibration curves of the first-generation and second-generation rolling sensors are compared in Figure 2.16. The second-generation rolling sensor has a higher resonant frequency than the first-generation rolling sensor. It also has a slightly flatter calibration curve in the region where the RDD measurements are made.

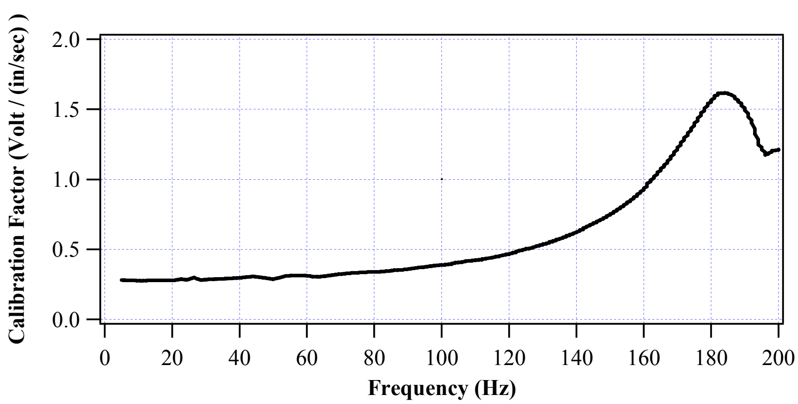

Figure 2.15 Magnitude Response of the Second-Generation Rolling Sensor Measured in the Calibration Setup Shown in Figure 2.13

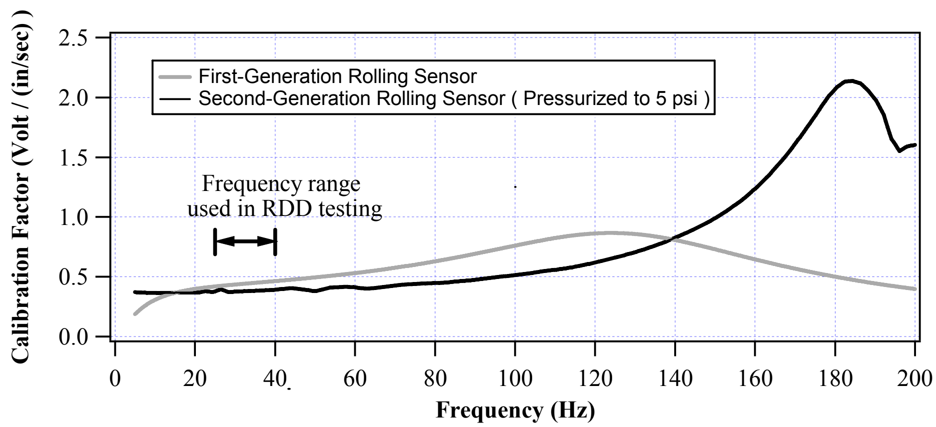

Figure 2.16 Comparison of the First-Generation and Second-Generation Rolling Sensors Calibration Curves

2.7 Design of the Air Pressuring System

Four second-generation rolling sensors were built, one with 9-in. (229-mm) diameter rolling wheels and three with 12-in. (305-mm) diameter rolling wheels. Each rolling sensor also has an additional hold-down force to maintain coupling with the pavement surface. Two rolling sensor designs were considered during this project. The design chosen has a polyurethane air spring to provide the required hold-down force.

The air springs on the second-generation rolling sensors were designed to maintain a pressure of roughly 5 psi (34.5 kPa) during RDD testing. Each air spring has a bottom area of 7 in^2 (45 cm^2). A 35-lb-hold-down force (156 N) is generated when the air spring is pressurized at 5 psi (34.5 kPa). To provide the hold-down force for the second-generation rolling sensor, each air spring needs to be pressurized by an external pressure source. The required air pressure can be obtained from the primary air compressor on the RDD truck. The primary air compressor on the truck is used mainly for operating the air-brake system and other pneumatic equipment. The primary air tank of the truck maintains a pressure of roughly 90 to 120 psi (621 to 827 kPa). This operation range in the RDD truck implies that a pressure relief valve will open when the pressure reaches 120 psi (827 kPa), and the air compressor will start running when the pressure inside the air tank drops below 90 psi (621 kPa).

In order to step-down the air pressure from the RDD primary air compressor to the required 5 psi (34.5 kPa) at each rolling sensor, an array of pressure regulators is needed to reduce the air pressure and to maintain it at the correct level throughout RDD testing. A new air pressuring system is proposed to meet the air pressure requirement of the second-generation rolling sensors. A system diagram of such a new pressuring system is shown in Figure 2.17.

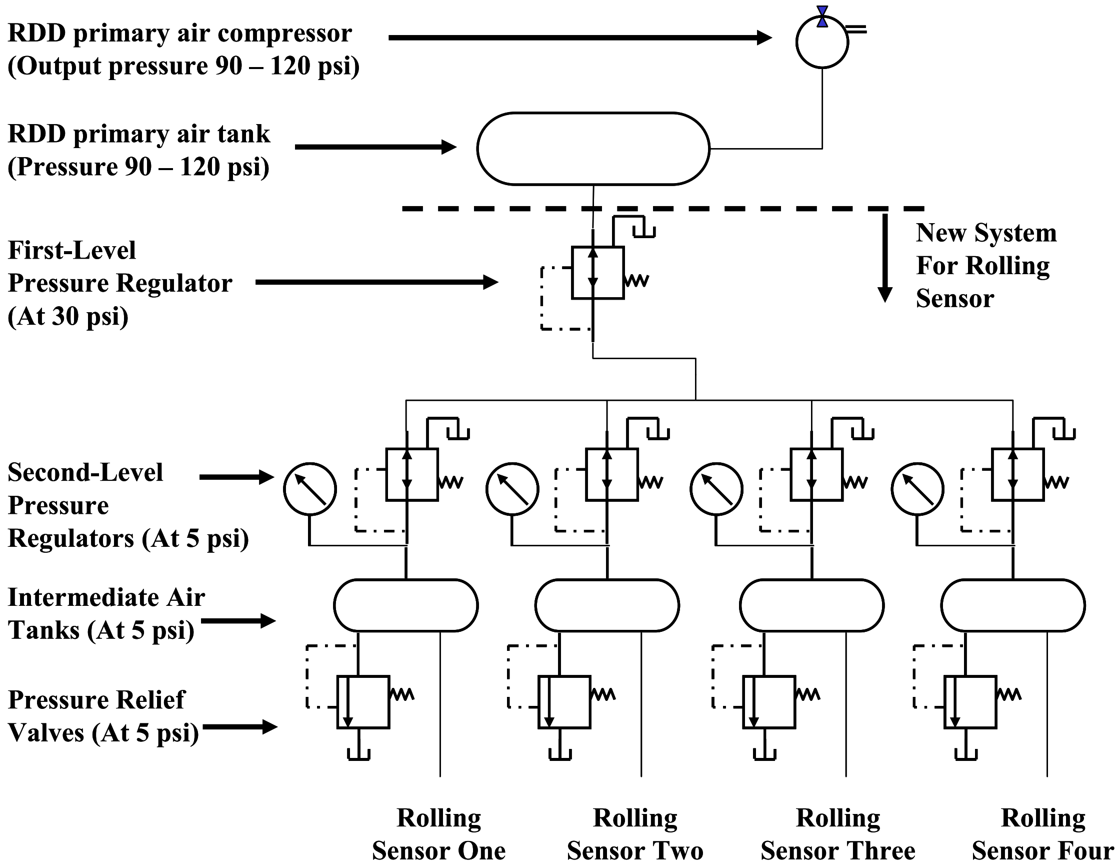

Figure 2.17 Schematic Drawing of the Air Pressuring System from the Primary RDD Air Compressor to Each Second-Generation Rolling Sensor

In the system diagram shown in Figure 2.17, two levels of pressure regulators are required to step-down the primary air compressor pressure from 90–120 psi (621–827 kPa) to 5 psi (34.5 kPa) at each air spring. One factor which controls the precision of a pressure regulator is the range of allowable input pressure of the regulator. Manufacturers of pressure regulators often have a selection of models with different input pressure ranges. In other words, a pressure regulator with a smaller input pressure range will have a more precise output pressure level in comparison with a pressure regulator with a larger input pressure range. Therefore, two levels of pressure regulators were chosen so that the precision of the output pressure level is not limited by the range of pressure between the main air compressor and the air springs of the rolling sensors.

The first-level pressure regulator reduces the main air-compressor pressure to around 30 psi (207 kPa). Then the output air pressure is distributed to four individual second-level pressure regulators. There are four pressure regulators in the pressure system that has been designed and constructed for the second-generation rolling sensors. Pneumatic Precision Regulators from Fairchild, Inc. (Model 10 Series) were chosen. Each one of these pressure regulators has an output pressure range of between 0 and 10 psi (0 and 69 kPa) and is located between the first-level pressure regulator and the intermediate air tanks. The sole purpose of these pressure regulators is to reduce the input air pressure of 30 psi (207 kPa) to the output air pressure of 5 psi (34.5 kPa). For practical purpose, these pressure regulators are presently mounted on a pressure panel box with an individual pressure gauge to monitor the pressure of each air spring. The pressure panel box is shown in Figure 2.18.

Figure 2.18 Photograph of the Pressure Panel Box Used to Provide a Constant 5 psi (34.5 kPa) Pressure to Each Second-Generation Rolling Sensor

Intermediate air tanks are connected downstream of the second-level pressure regulators. The intermediate air tanks act as buffer zones to minimize the change of pressure inside each air spring when the volume of the air spring changes due to changes in pavement profile. Pressure fluctuation inside the air spring will be further discussed in the next section. Each intermediate air tank is connected to the air spring and a pressure relief valve is also fitted on each intermediate air tank to prevent any accidental pressure surge that can damage the polyurethane air springs. These pressure relief valves are the poppet-type relief valve, and the relief pressure setting is controlled by turning the top cap, which changes the length of a calibrated compression spring. A prototype towing frame, pressure system, and two second-generation rolling sensors are shown in Figure 2.19. This prototype towing frame can support only two rolling sensors. Therefore, only two rolling sensors were used during the field evaluation study presented in Chapters 3, 4 and 5. To support four rolling sensors, a towing frame and pressure system would be about two times greater in length and have four intermediate air tanks.

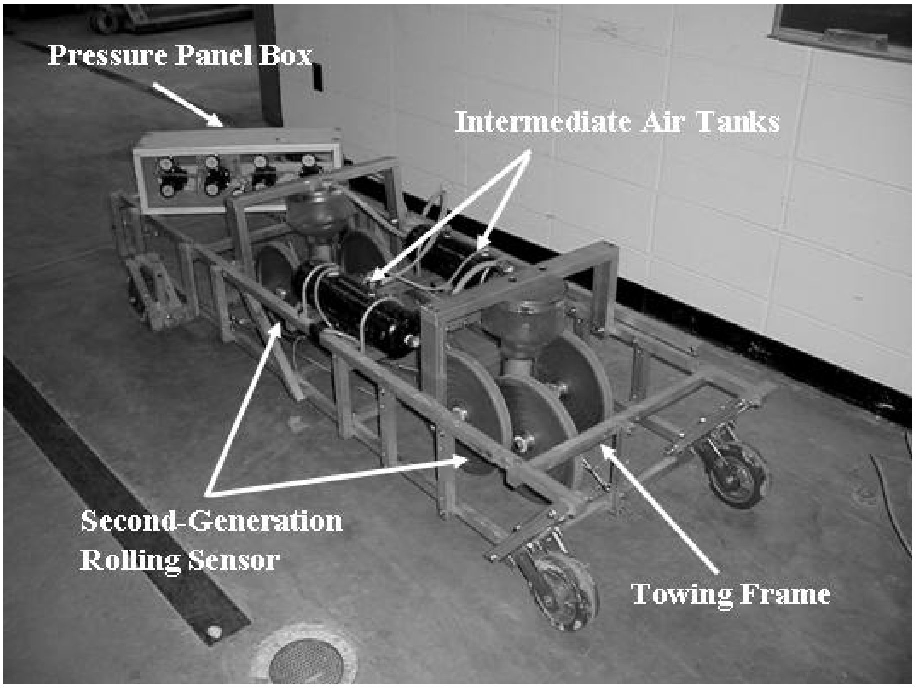

Figure 2.19 Photograph of a Prototype Towing Frame and the Pressuring System that Supports Two Second-Generation Rolling Sensors

2.8 Minimizing Hold-Down Pressure Fluctuation

The second-generation rolling sensors rely on the applied hold-down force to maintain coupling with the pavement surface at testing speeds above 1 mph (1.6 km/hr). The hold-down pressure within the air springs can adversely influence the maximum testing speed achievable by the second-generation rolling sensors. There are many factors that can cause pressure fluctuations inside the air springs. Some of these factors are: (1) pressure variability that is caused by fluctuations in supply pressure, (2) volume change of the compressed air inside the air springs due to pavement surface-profile variations, and (3) any air leakage along the pressure lines. Each of these factors is discussed below, and features of the pressure system are also described.

First, the supply pressure of the system will never be constant. The pressure regulators use the balanced-force principle to regulate the output pressure, and these regulators have a small output pressure range of 1 to 10 psi (6.9 to 69 kPa). This type of regulator has a calibrated compression spring inside which connects to the top of a diaphragm. This compression spring controls the output pressure by balancing the forces that act on both sides of the diaphragm. Furthermore, any excessive pressure will bleed to the atmosphere through a pressure-relief port. The accuracy of the output pressure depends on the response of the compression spring, and a softer spring is used for lower-pressure-range regulators. The length of a soft spring displaces more than a stiff spring under a given pressure increment, and more displacement often means more control on the accuracy of the output pressure.

Second, Boyle's Law states that there is a fixed relationship between the pressure and the volume. The pressure of a gas decreases as the volume of that gas increases. Boyle's Law can be represented by:

$$p\,V = kT \tag{2.3}$$

where

p = pressure of gas
V = volume of gas
k = constant
T = temperature of gas

As a second-generation rolling sensor rolls along the pavement, the varying profile of the pavement surface can change the overall height of the rolling sensor. This change in height occurs from the compression or extension of the air spring that is located at the top of each rolling sensor. As the rolling sensor rolls across an overlay section that suffers from severe rutting distress, the height of the rolling sensor will increase and therefore also increase the gas volume of the air spring. This change will correspondingly decrease the pressure inside the air spring, according to Boyle's Law. Since it is impossible to predict how the volume of the air spring will change, an intermediate air tank is installed for each sensor to compensate for air spring pressure fluctuations.

These intermediate air tanks are made from a 4-inch (102 mm) diameter steel pipe section. They act as a buffer zone downstream of each second-level pressure regulator. Two intermediate tanks were installed; each will compensate for the pressure fluctuations in each rolling sensor. These tanks are conveniently located on the towing frame that is in the closest position to the associated rolling sensor. By providing a large volume buffer, it is expected that any change in the air-spring volume will not significantly affect the pressure within each air spring. Furthermore, the air passage between each rolling sensor and the corresponding intermediate air tank are provided using 0.5-in. (12.7-mm) diameter polyethylene lines. This size line is larger in diameter than the air lines for the rest of the pressure system. By locating an intermediate air tank close to each rolling sensor and by having larger diameter air lines, it is possible to achieve nearly unrestricted flow for compensating any air-spring pressure fluctuations.

Third, at the current configuration, a pressure regulator is used to regulate the pressure of each air spring. There are two main reasons for this configuration: (1) to allow the testing crew to monitor the pressure of each air spring, and (2) to provide continuous operation of the other three rolling sensors if one of them experiences problems in the field. Furthermore, this system can easily be re-configured so that a single regulator can be used to control more than one rolling sensor. This arrangement is useful if there are air leakages within the pressure system during the field testing, and this configuration provides a potential backup system.

2.9 Summary

The primary objective of this research project is to increase the RDD testing speed from 1.0 mph (1.6 km/hr) to 3.0 mph (4.8 km/hr). The only technical hurdle to accomplishing this objective is developing new rolling sensors, called second-generation rolling sensors. The two major factors that need to be improved in developing the second-generation rolling sensor are: (1) increase the hold-down force on the sensor so that it does not decouple from the pavement when traveling at 3 mph (4.8 km/hr), and (2) decrease the level of rolling noise. An air spring system was developed to increase the hold-down force and larger wheels were built to decrease the level of rolling noise. The paths followed to develop these improvements are discussed in this chapter. The final design and constructed rolling sensors are presented. The performance of the second-generation rolling sensors is presented in Chapters 3 to 5.

Chapter 3. Field Evaluation of the Second-Generation Rolling Sensor Performance: Rolling Noise

3.1 Introduction

The design and construction of the second generation of rolling sensors was discussed in Chapter 2. In this chapter, the performance of the second-generation rolling sensor is evaluated and compared with the first-generation rolling sensor. The rolling sensor is a key component in RDD testing. It is a contact-type sensor which rolls along the pavement surface to measure the dynamic deflections of the surface. Rolling noise is generated as the rolling sensor moves along a pavement surface.

Rolling noise during testing and decoupling of the rolling sensor from the pavement are critical design aspects affecting the performance of rolling sensors. The first of these two aspects, rolling noise, is discussed in this chapter. First, background information concerning rolling noise is presented. This discussion focuses on the source of rolling noise and some desirable characteristics of rolling noise during RDD testing. Next, the benefits of having rolling noise that is low-level and has frequency content away from the RDD operating frequency range are presented. Rolling noise with such characteristics allow better time-frequency resolution digital filters to be used to filter out the rolling noise. Then laboratory evaluation of noise transmission through the air spring is also presented. Last, the rolling noise characteristics of the second-generation rolling sensor are presented using data collected during preliminary field trials performed on a flexible pavement at UT's Pickle Research Campus.

3.2 Background Information Concerning Rolling Noise

Every possible attempt should be made to minimize RDD measurement noise. In particular, the rolling sensor signal always contains some noise during RDD testing. Furthermore, this rolling noise tends to increase as the test speed increases. During the design process of the second-generation rolling sensor, noise minimization has always been an important consideration. As a result, noise minimization is reflected in the design of the second-generation rolling sensor. This includes its frequency response, its rolling wheel geometry, and the use of an air spring to provide an additional hold-down force.

The sources and characteristics of rolling noise are discussed below. First, the sources of rolling noise are discussed. For the second-generation rolling sensor, there are two main rolling noise sources. These sources are: (1) the rolling action of the sensor, and (2) noise transmitted through the air spring and the towing frame. The desired characteristics of rolling noise and the selection of a digital filter to filter out rolling noise are then discussed.

3.2.1 Sources of Rolling Noise

Noise from Rolling Action of the Sensor on the Pavement—As long as the RDD uses contact-type sensors for making deflection measurements, noise from physical rolling of the sensor on the pavement surface will always exist. The roughness of the pavement will inevitably generate noise, and the rolling noise can be overwhelming at times if the rolling sensor rolls over very rough surfaces. The geometry of the second-generation rolling sensor was designed to minimize the rolling noise by having polyurethane coating on the rolling wheels and by having larger-diameter rolling wheels. Furthermore, using three rolling wheels with different offsets allows cancellation of random noises. These design issues were discussed in Chapter 2.

Noise Transmitted through the Air Spring and the Towing Frame—A major difference between the first-generation rolling sensor and the second-generation rolling sensor is that the second-generation sensor has an air spring attached to the top of the rolling carriage. The air spring has two main functions. First, it provides a hold-down force to improve the coupling between the rolling sensor and the pavement surface. Different levels of hold-down force can be applied by simply changing the air pressure inside each air spring. Second, the air spring isolates vibrations transmitted from the towing frame to the rolling sensor. This second function is just as important as the first because vibration that is close to the chosen RDD operating frequency can be transmitted through the towing frame to the rolling sensor. This source can have a detrimental effect on the RDD deflection measurements. A laboratory study was carried out to evaluate the transmission of noise through the air spring and the findings are presented below.

3.2.2 Desirable Characteristics of Rolling Noise

Rolling noise can be regarded as a random process which is primarily controlled by the testing speed and the diameter of the wheels mounted on each rolling sensor. In general, rolling noise increases with increasing testing speed. Also, a rolling sensor with larger diameter wheels generates a lower noise level than a rolling sensor with smaller diameter wheels when rolled over a pavement at the same speed. The two main improvements in the second-generation rolling sensor are the additional hold-down force and larger diameter wheels. These improvements allow RDD deflection profiles to be collected at higher speeds in a quieter environment. The desired characteristics of rolling noise are listed as follows.

1. It is more desirable to have a low level of rolling noise when compared with the RDD signal. This noise level yields a higher signal-to-noise ratio (SNR). A detailed discussion is presented in Section 3.2.3.
2. It is more desirable to have rolling noise that is evenly distributed across the frequency domain than concentrated rolling noise near the RDD operating frequency. A detailed discussion is presented in Section 3.2.4.
3. It is more desirable to have rolling noise located far away from the RDD operating frequency in the frequency domain. This noise distribution improves the time (or spatial) resolution of the digital filter. A detailed discussion is presented in Section 3.2.5.

The steps used to process the RDD deflection signal from the rolling sensor are summarized in Figure 3.1. In the first step, the raw RDD rolling sensor signal is demodulated by multiplying the signal with Equation 3.1:

$$\cos 2\pi f_o t + i \sin 2\pi f_o t \tag{3.1}$$

where

f_o= RDD operating frequency,
t = time, and
i = complex number operator ($\sqrt{-1}$).

This shifts the RDD signal from the operating frequency to 0 Hz in the frequency domain. In the second step, a notch-pass digital filter is applied to isolate the demodulated RDD signal at 0 Hz from noise at other frequencies. The design of this digital filter affects the deflection measurement significantly. In the third step, a constant factor is applied to convert the geophone voltage measurement to the displacement in the complex number domain. In the fourth step, the pavement displacement is determined using the square root of the sum of squares of the real and imaginary parts of the complex number solution.

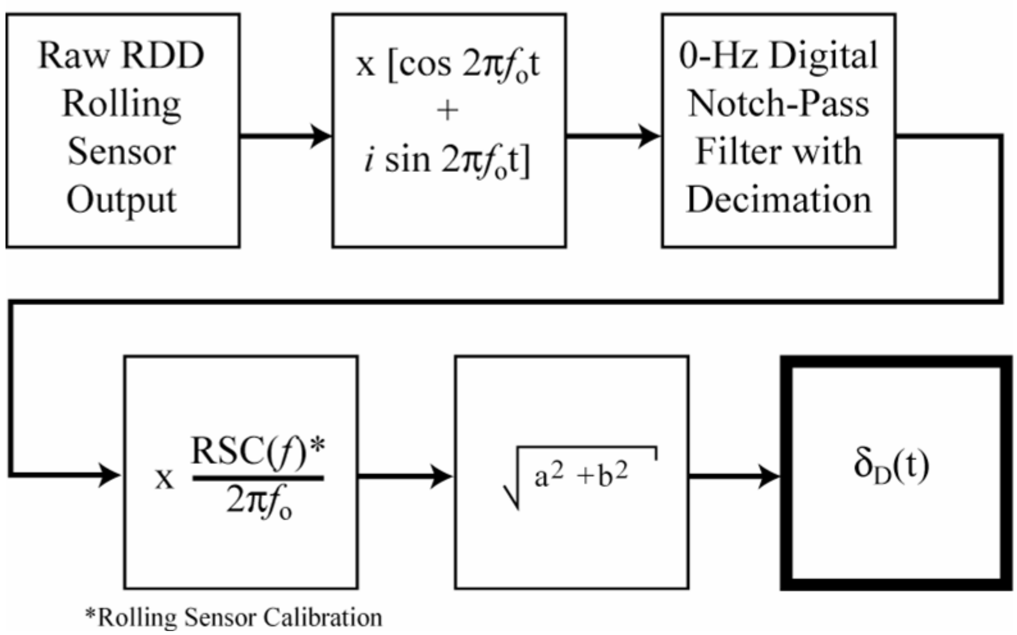

Figure 3.1 Flow Diagram of Procedure Used to Calculate Dynamic Displacement from the RDD Rolling Sensor Output (from Bay et al., 1998)

3.2.3 Level of Rolling Noise

In the context of this work, rolling noise refers to energy measured outside the frequency in which the RDD loading rollers excite the pavement. Since the RDD applies sinusoidal dynamic loading at a single frequency, it is more convenient to investigate the level of rolling noise in the frequency domain. A common term used to describe noise embedded in a signal measurement is *averaged noise level*.

Figure 3.2 illustrates the benefit of reducing the rolling noise level in the RDD measurement using synthesized data. In Figure 3.2(a), the RDD signal is at 35 Hz and a noise component with the same amplitude is located at 80 Hz. If a finite impulse response (FIR) filter is designed to attenuate the 80-Hz noise component to -30 dB, the digital filter would require 109 filter coefficients. In Figure 3.2(b), the noise level at 80 Hz is -10 dB below the RDD signal at 35 Hz. As a result, a digital filter with 85 filter coefficients is required to attenuate the 80-Hz noise component to -30 dB. Similarly, the noise level at 80 Hz is further reduced to -20 dB below the RDD signal level as shown in Figure 3.2 (c). Then, a FIR filter with only 63 filter coefficients is needed.

To summarize, a low noise level measurement requires a digital filter with only moderate attenuation to attenuate stop-band frequencies to the desired level. It follows that a digital filter with moderate attenuation will have a smaller number of filter coefficients if the noise level in the stop band is less. In general, a FIR digital filter with a higher number of filter coefficients often has poorer time resolution (i.e., poor spatial resolution in the RDD continuous deflection profile).

<table>
<tr><td rowspan="3">(a)</td><td>Signal: 35-Hz at 0 dB
Noise: 80-Hz at 0 dB</td><td rowspan="3">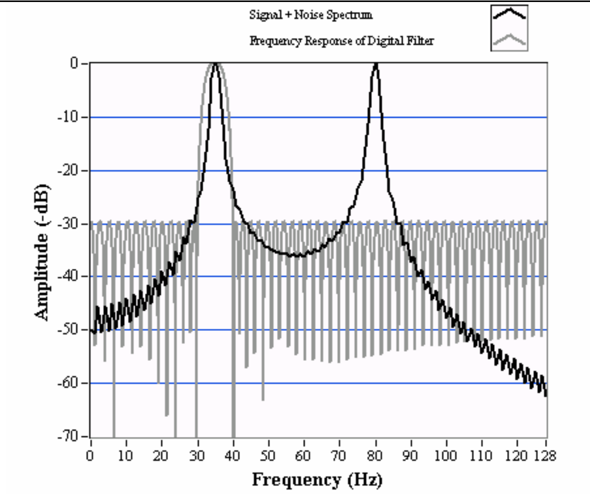
</td></tr>
<tr><td>Required Stop-Band
Attenuation = -30 dB</td></tr>
<tr><td>Number of FIR Filter
Coefficients = 109</td></tr>
<tr><td rowspan="3">(b)</td><td>Signal: 35-Hz at 0 dB
Noise: 80-Hz at -10 dB</td><td rowspan="3">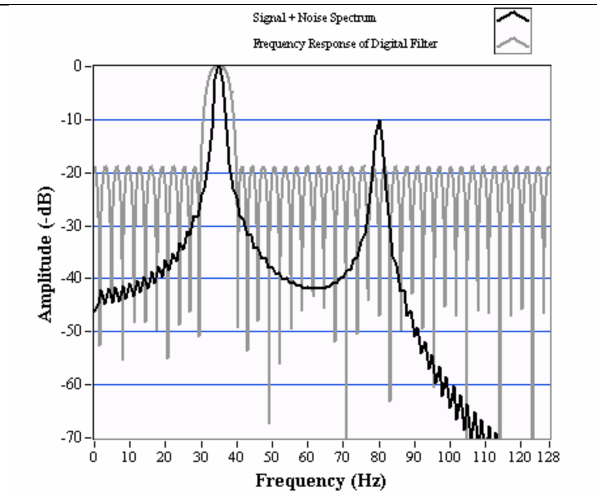
</td></tr>
<tr><td>Required Stop-Band
Attenuation = -20 dB</td></tr>
<tr><td>Number of FIR Filter
Coefficients = 85</td></tr>
<tr><td rowspan="3">(c)</td><td>Signal: 35-Hz at 0 dB
Noise: 80-Hz at -20 dB</td><td rowspan="3">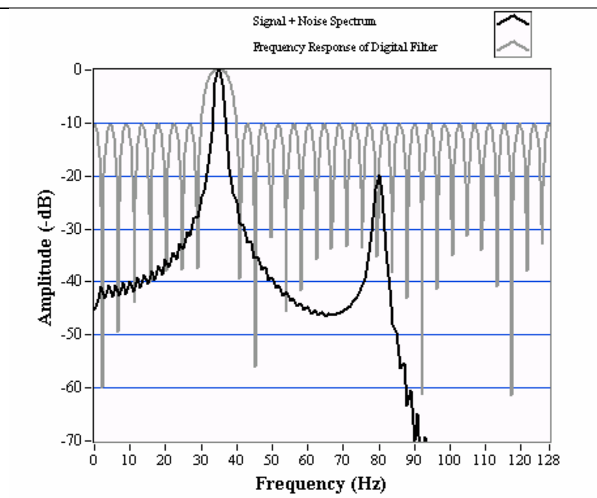
</td></tr>
<tr><td>Required Stop-Band
Attenuation = -10 dB</td></tr>
<tr><td>Number of FIR Filter
Coefficients = 63</td></tr>
</table>

Figure 3.2 (a), (b), and (c). Attenuation Levels and Number of FIR Filter Coefficients of Different Digital Filters to Remove a Noise Component at 80-Hz

3.2.4 Frequency Content of Rolling Noise

The next factor that controls the performance of a digital filter is the frequency content of the rolling noise. Since the RDD outputs a sinusoidal dynamic force at a single frequency, then the precise input frequency is known. This fact allows the design of an effective digital filter to filter out rolling noises at frequencies other than the RDD operating frequency. In general, a more demanding filter is required if a sharp transition band is needed to distinguish between pass-band and stop-band frequencies. The primary reason for using a notch-pass filter with a sharp transition band is to ensure that no rolling noise that is located close to the operating frequency is allowed to pass through the digital filter. By the same token, the distribution of the rolling noise in the frequency domain governs a particular digital filter design if an optimal digital filter design is pursued.

The RDD signal and different types of synthetic rolling noises are illustrated in Figure 3.3. In each case, the synthetic rolling noise has a different distribution in the frequency domain. In Figure 3.3(a), the RDD is superimposed with a low level of uniformly distributed rolling noise. In Figure 3.3(b), the RDD signal is superimposed with a moderate level of uniformly distributed rolling noise. In Figure 3.3(c), the RDD signal is superimposed with a "1/f-type" of rolling noise. The amplitude of this type of noise decreases with increasing frequency. If an optimal digital filter design is pursued, a digital filter should be chosen according to the distribution of the rolling noise measurement.

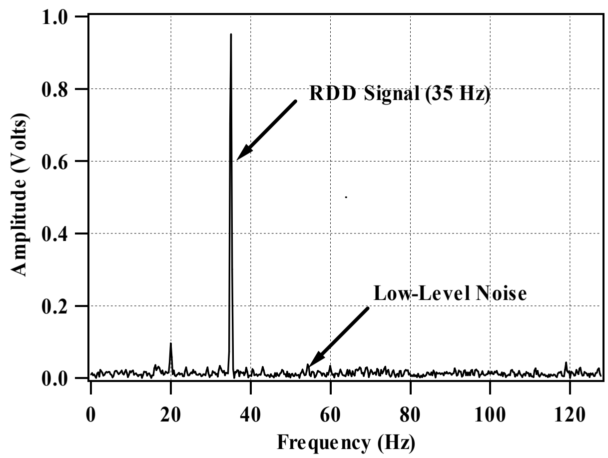

(a) RDD signal and low level of uniformly distributed rolling noise

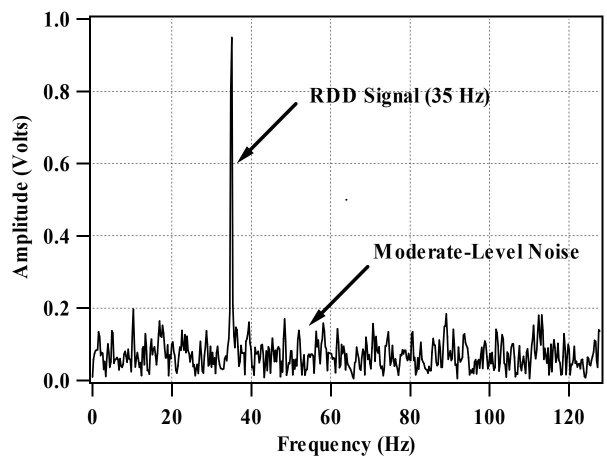

(b) RDD signal and moderate level of uniformly distributed rolling noise.

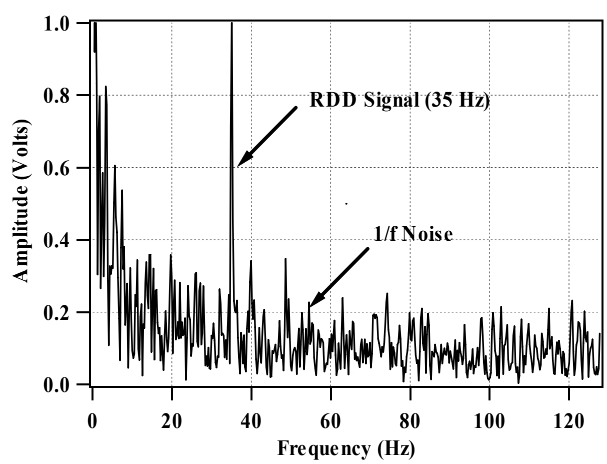

(c) RDD signal and non-evenly distributed rolling noise. *This type of noise is commonly known as the 1/f noise, which has decreasing amplitude with increasing frequency.*

Figure 3.3 (a), (b), and (c). RDD Signal and Different Types of Synthetic Rolling Noise

3.2.5 Noise Removal—Digital Signal Processing

As discussed earlier, the raw measurement from the RDD rolling sensors contain both the RDD signal component at the chosen operating frequency and different noise components. Assuming the pavement is a linear system, the pavement response (measured deflection) will be at the same frequency as the loading that was used to excite the pavement (RDD sinusoidal load at the chosen operating frequency). Any frequency components that are not located at the RDD operating frequency are assumed to be unwanted noise. For the RDD to measure the surface deflection correctly, specially-designed digital filters are applied to the raw measurement to resolve the amplitude envelope of the deflection signal. It is important to select a digital filter to filter out noise in the raw measurement. Theoretically, a digital filter with an infinitely narrow pass band (i.e., excellent frequency resolution) should be chosen so that any noise outside the RDD operating frequency is removed from the time record. However, this approach is not practical because such filter would require averaging over an infinitely long time record (i.e., poor time resolution). This point is best illustrated in the example shown in Figure 3.4, which contains three scenarios using different digital filters to remove noise from the raw RDD measurement.

In Figure 3.4(a), a pure 35-Hz sinusoidal waveform was synthesized in a 2-second duration time record. This signal in the time domain represents the signal from a rolling sensor where no noise is present (i.e., the RDD is in stationary mode). This waveform has an amplitude of 2 between 0 and 1 second, and the amplitude drops to 0 instantly between 1 and 2 seconds. Since there is no noise present inside the Nyquist frequency band (i.e., 0–128 Hz), almost any low-pass filter with a cutoff frequency higher than 35 Hz can resolve the 35-Hz signal. The amplitude envelope of the filter output is also shown. This digital filter has a very wide pass band (i.e., poor frequency resolution), yet it has a very fast response in the time domain (i.e., excellent time or spatial resolution). The filtered output in the time domain shows a peak amplitude versus time just like the input record.

In Figure 3.4(b), the same 35-Hz sinusoidal waveform is chosen as the input. However, a 100-Hz sinusoidal waveform is also superimposed to simulate a noise component at 100 Hz. A digital filter with a moderate pass band and a moderate response time is chosen to remove the 100-Hz noise component. This digital filter satisfies the time and frequency resolution requirement with ease because the signal and noise component are separated far away in the frequency domain. Therefore, the filtered output in the time domain shows a peak amplitude versus time, which slightly smears the time record near the sharp amplitude transition from 1 to 0.

In Figure 3.4(c), the same 35-Hz sinusoidal waveform is superimposed with a 30-Hz sinusoidal waveform. A digital filter with narrow pass band is needed to filter out the 30-Hz noise component due to the fact that the signal component and the noise component are located close to one another in the frequency domain. The shortcoming of having a narrow digital filter is a slow response time, which effectively decreases the ability to detect sharp changes in deflection values along the continuous deflection profile. It is apparent in Figure 3.4 that there is always a trade-off between the two resolutions: (1) frequency resolution (accurately identifying the pavement deflection), and (2) time resolution (accurately identifying localized pavement features such as crack or joint).

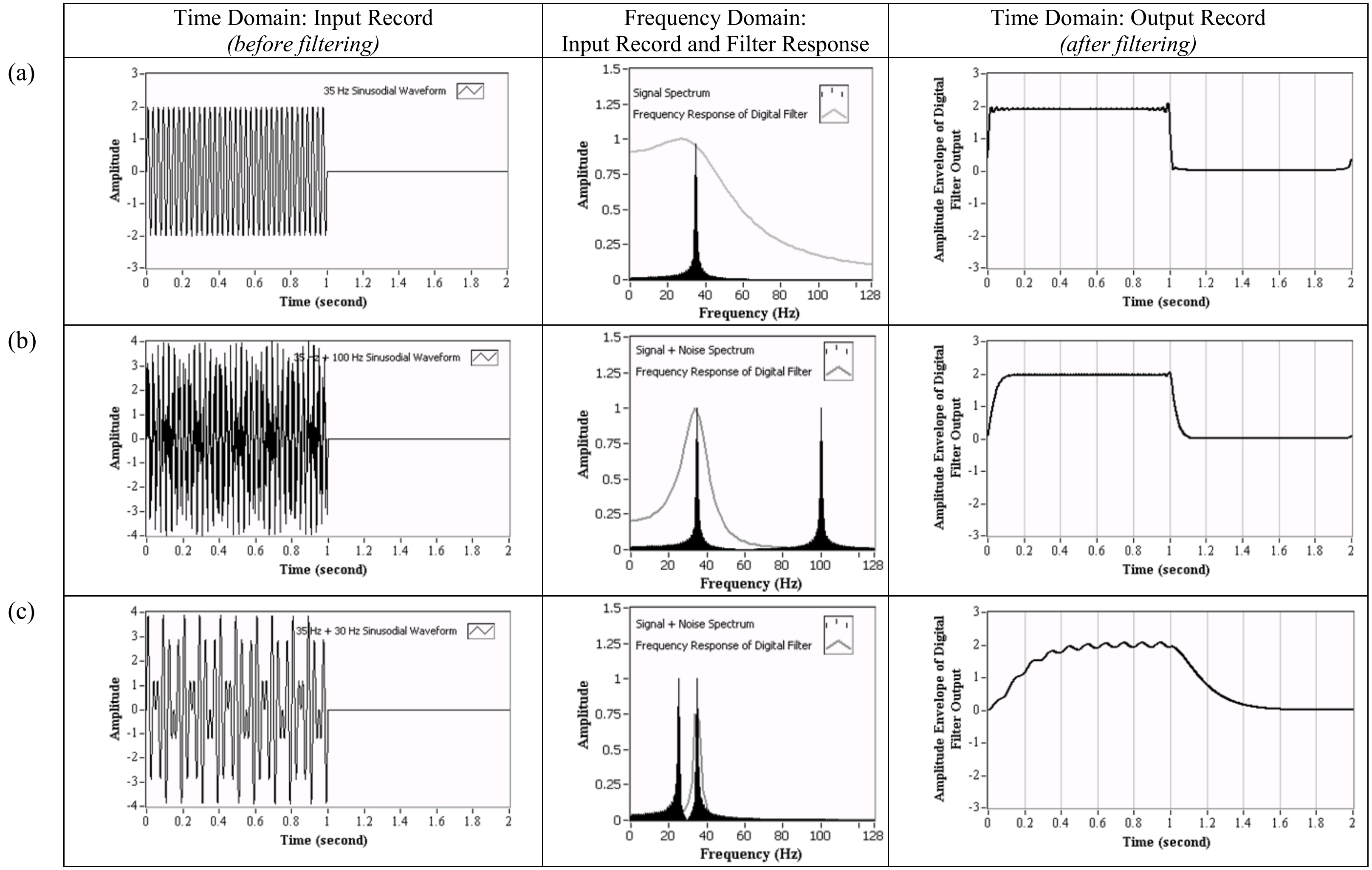

Figure 3.4 (a), (b), and (c). Time and Frequency Responses of Different Digital Filters to Resolve a 35-Hz Sinusoidal Signal

3.3 Laboratory Evaluation of Noise Transmission through the Air Spring

To evaluate the noise isolation performance of the air spring, two identical accelerometers, Model 736T by Wilcoxon, Inc., are attached above and below the air spring. Then an impact force was applied using a rubber mallet hammer. The output signal from each accelerometer was recorded using an Agilent dynamic signal analyzer, Model 35670A. A photograph of the noise evaluation setup is shown in Figure 3.5. The time histories from the two accelerometers are shown in Figure 3.6. The difference in acceleration after the impact wave travels through the air spring (pressurized at 5 psi, which is equivalent to 35 lb hold-down force) has a ratio of approximately 1:60. This is equivalent to a measurement error of 0.17 mils due to noise transmission through the air-spring when the rolling sensor is tested on a pavement with an average deflection of 10 mils. Therefore, the air spring is believed to sufficiently reduce noise that might be transmitted to the rolling sensor from the towing frame. In future studies, acccelerometers will be placed on the carriage of the rolling sensor and on the towing frame immediately above the air spring to quantify the attenuation characteristics of the air-spring.

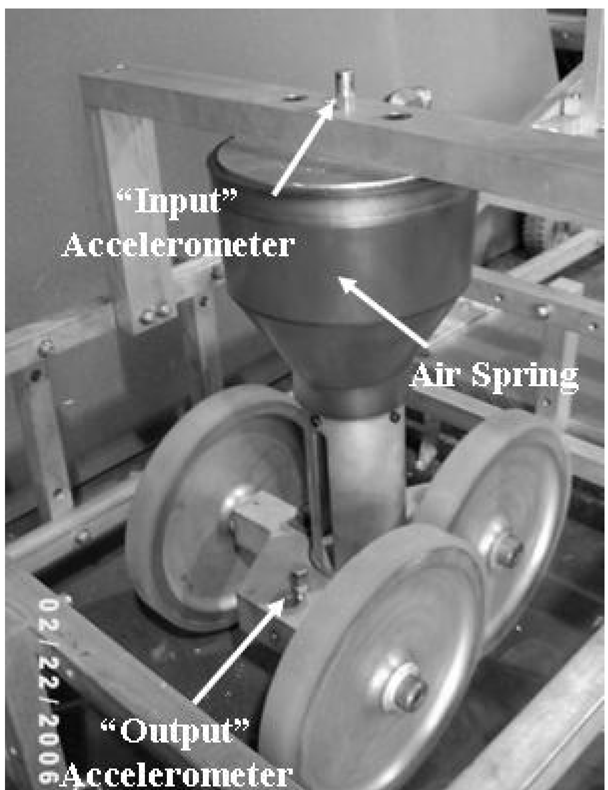

Figure 3.5 Photograph of the Setup Used to Evaluate the Noise Isolation Performance of the Air Spring

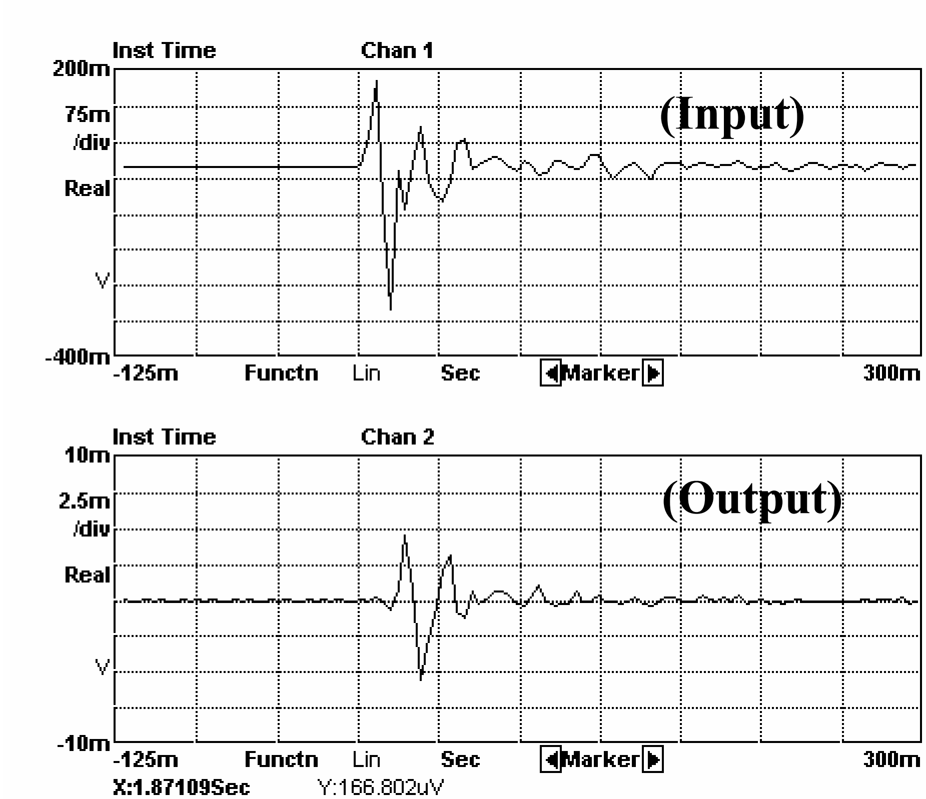

Figure 3.6 Output from Accelerometers Located Above (Input) and Below (Output) the Air Spring

3.4 Rolling Noise Evaluation—Preliminary Field Trials without the RDD Truck

After the second-generation rolling sensor was built and calibrated in the laboratory, preliminary field trials were performed on a short section of flexible pavement at the Pickle Research Campus (PRC). A photograph of the test site is shown in Figure 3.7. The asphalt concrete (AC) pavement is rough in this section. The primary goals of these trials were to evaluate the rolling noise of the second-generation rolling sensor and to compare the performance of the first-generation rolling sensor with 6-in. (152-mm) diameter wheels to the performance of the second-generation rolling sensor with 12-in. (305-mm) diameter wheels. No RDD loading was required during the preliminary field trials. As discussed in Sections 2.1.1 and 2.1.2, there are two criteria for evaluating the performance of the rolling sensor. The maximum testing speed achievable before a rolling sensor uncouples from the pavement surface is one criterion. The level of rolling noise embedded in the rolling sensor measurement is the second criterion. Both criteria will determine if the second-generation rolling sensor will be able to measure pavement surface deflection at the 3 mph (4.8 km/hr) target, and whether the digital band-pass filter can resolve the amplitude at the chosen RDD operating frequency accurately.

By simply towing the rolling sensor assembly along the test path manually, it is easy to maintain a reasonably constant speed and the possibility of any noise transmitted from the RDD truck and the loading rollers to the rolling sensor can be entirely eliminated. Figure 3.8 is a photograph of the test setup. A first-generation rolling sensor (with 6-in. (152-mm) diameter rolling wheels) and a second-generation rolling sensor (with 12-in. (305-mm) diameter rolling wheels) are attached to a towing frame. Air pressure is supplied to the pressure panel box from a portable air compressor via an air hose. The speed and distance traveled are recorded using a distance measuring instrument (DMI), which is attached to the back of the towing frame. An on-board data acquisition system and a laptop computer were used to record the signals from each rolling sensor and the DMI unit. The entire assembly unit was being towed by hand along the test path with different average speeds and at different hold-down pressures. This same setup will also be used to evaluate the decoupling performance of the second-generation rolling, which is presented in Chapter 4.

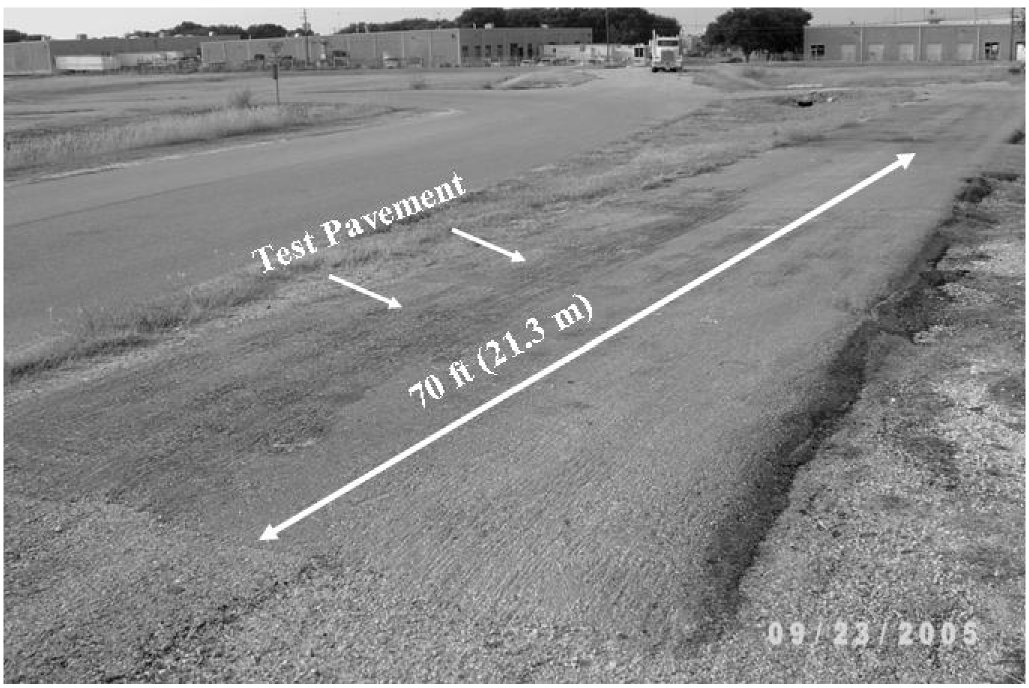

Figure 3.7 Photograph of Flexible Pavement at Pickle Research Campus where Field Tests of Rolling Noise Were Performed

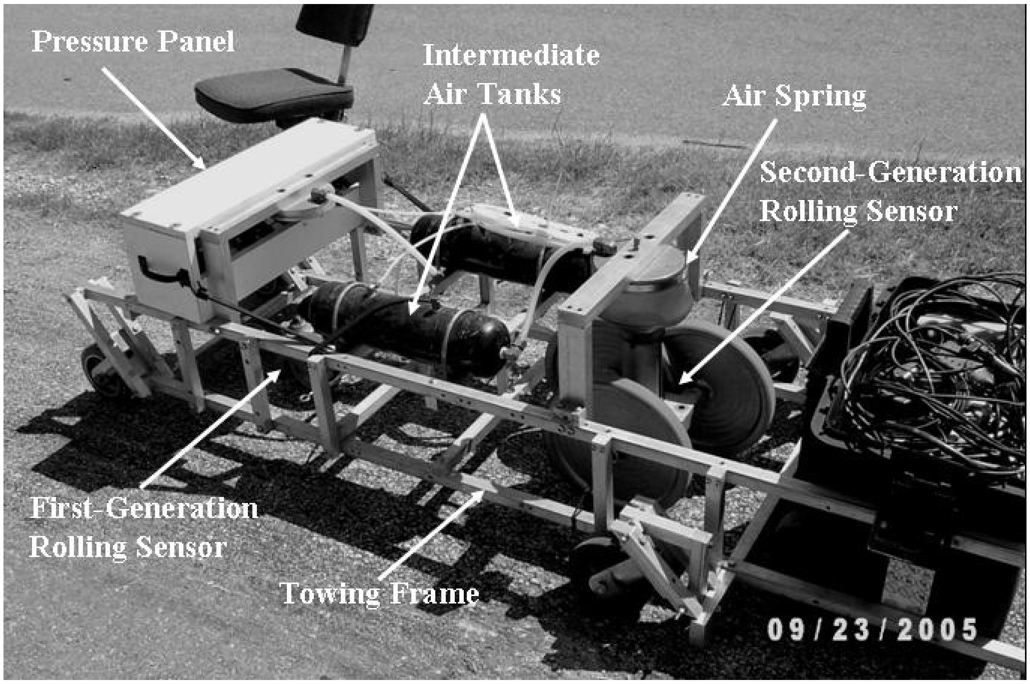

Figure 3.8 Photograph of the Test Setup of the First- and Second-Generation Rolling Sensors in a Towing Frame

3.5 Level and Frequency Content of Rolling Noise

The general relationship between the average measured noise level and the average testing velocity for the first-generation and second-generation rolling sensor is shown in Figure 3.9. This field measurement was collected along a rough flexible pavement (TxMLS temporary pad), using the first- and second-generation sensors in the same towing frame (Figure 3.8). The second-generation had 12-in. (305-mm) diameter rolling wheels. Using the setup shown in Figure 3.8, a 35-lb (16-kg) hold-down force was applied when the measurements were performed. As predicted for both rolling sensors, the average noise floor increases with increasing testing velocity. More importantly, it was shown that the average noise floor in the RDD operating frequency range (i.e., 25–40 Hz) of the second-generation rolling sensor is about 50% less than the first-generation rolling sensor, when tested at approximately 3 mph (4.4 fps). A similar trend was observed when the first-generation rolling sensor was tested on different highway project-level studies. As seen in Figure 3.9, considerable variability exists in these measurements, most likely due to variability in pavement roughness even for this flexible pavement site (which was very rough).

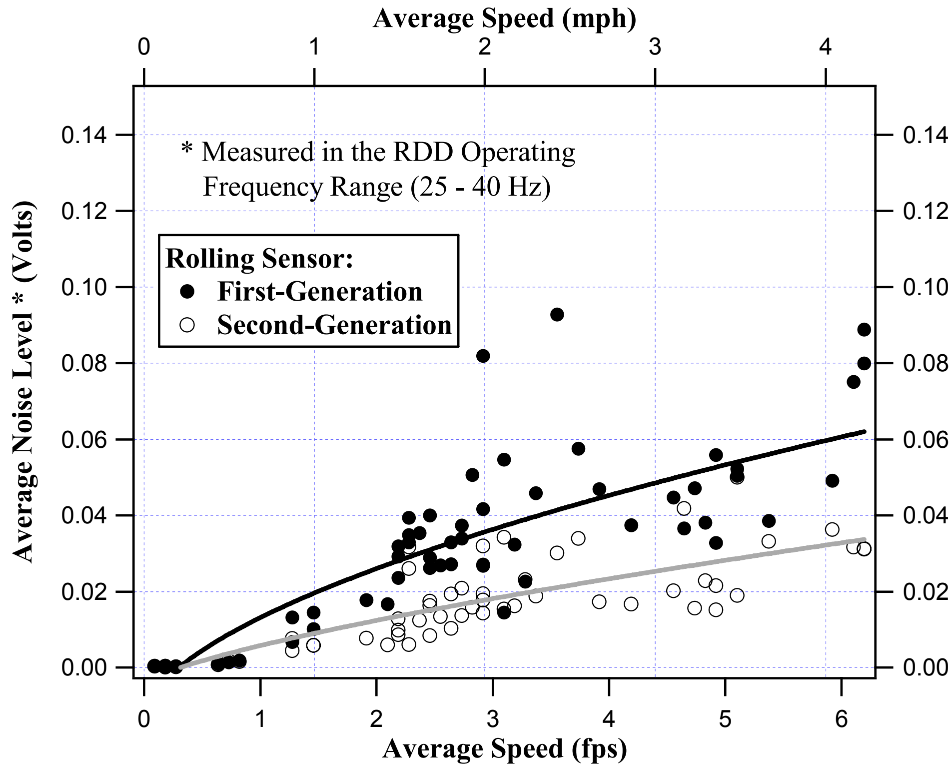

Figure 3.9 General Relationship Between Average Noise Level and Average Test Velocity for First-Generation and Second-Generation Rolling Sensors

The level and frequency content of the rolling noise can be investigated by plotting the power spectrum of the first-generation and second-generation rolling sensors. Comparisons using the results from the preliminary field trials for both the first-generation and second-generation rolling sensors are presented in Figures 3.10 to 3.15. In these figures, power spectra collected at different test velocities are shown. In terms of the measured rolling noise, the noise power spectrum of the second-generation rolling sensor is consistently smaller than the noise power spectrum of the first-generation rolling sensor in the RDD operating frequency range (25 to 40 Hz). It can also be observed that the magnitude of the power spectrum in the operating frequency range generally increases with increasing testing speed, except for the case in Figure 3.13, where the power spectrum is larger than the ones shown in Figures 3.14 and 3.15. Since the power spectrum is influenced by the speed and roughness of the pavement, the results in Figure 3.13 are likely explained by the random characteristics of road roughness at the time the measurements were made (levels of roughness varied at different locations).

This comparison shows that the second-generation rolling sensor significantly reduces the level of rolling noise in the RDD measurement. Furthermore, the noise power spectrum of the second-generation rolling sensor is more evenly distributed in the frequency domain than the first-generation rolling sensor. Of particular importance is the reduced level of rolling noise in the RDD testing frequency range (i.e., 30–45 Hz).

From the preliminary field trials, it was found that the second-generation rolling sensor performs much better than the first-generation rolling sensor in terms of the level and frequency content of the measured rolling noise. It should be noted that these data were collected on a flexible pavement, and differences in results are expected on other types of pavement with different roughness. In particular, rough, jointed rigid pavements will have higher rolling noise.

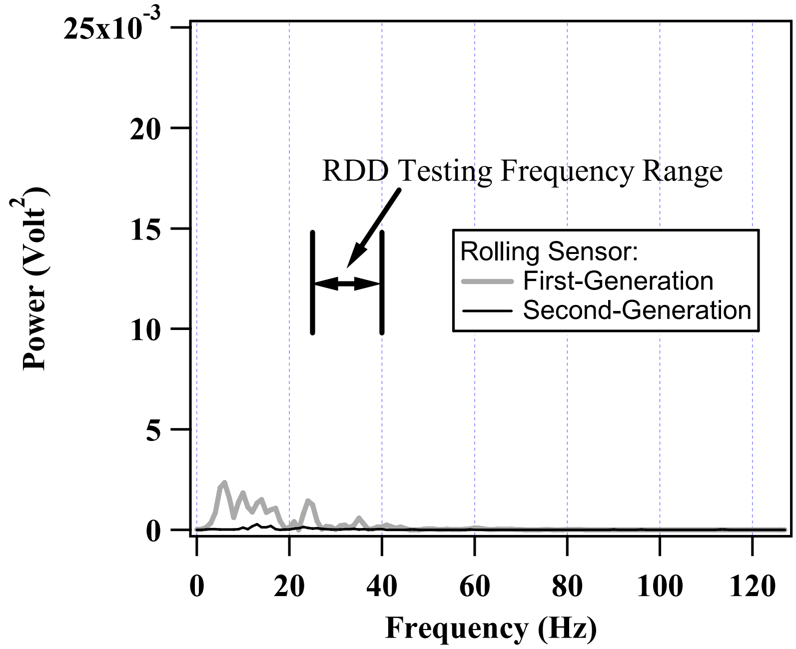

Figure 3.10 Power Spectra of the First-Generation and Second-Generation Rolling Sensors at a Testing Velocity of 1 mph (1.5 ft/sec)

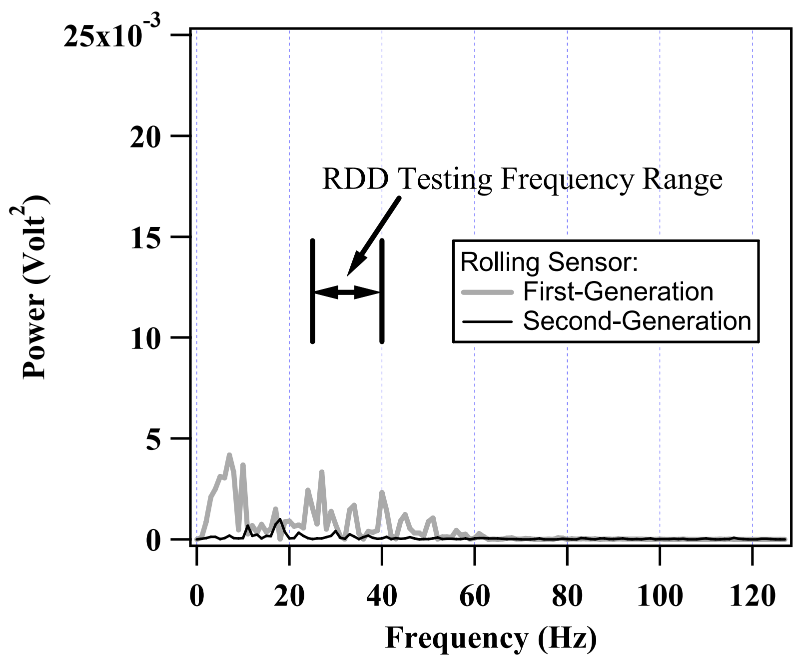

Figure 3.11 Power Spectra of the First-Generation and Second-Generation Rolling Sensors at a Testing Velocity of 1.6 mph (2.3 ft/sec)

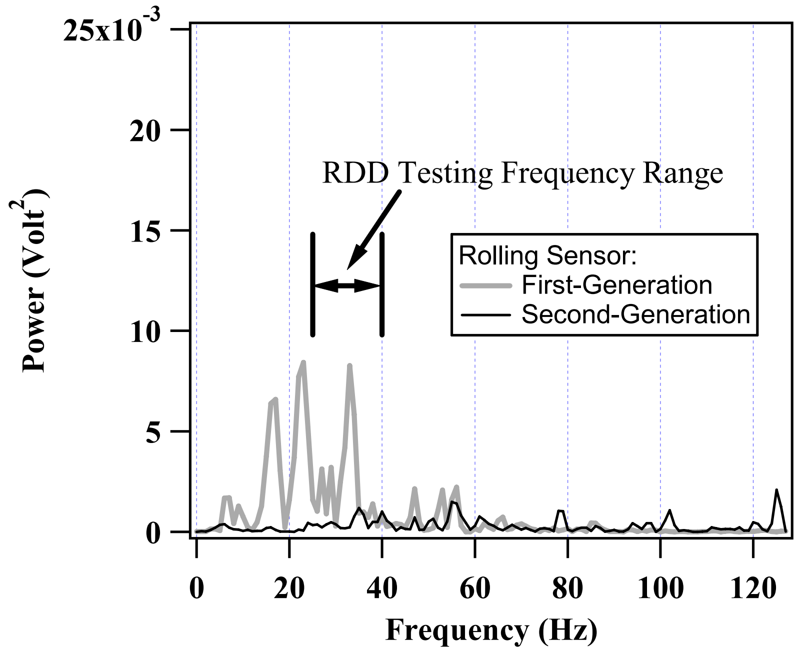

Figure 3.12 Power Spectra of the First-Generation and Second-Generation Rolling Sensors at a Testing Velocity of 2.7 mph (4.0 ft/sec)

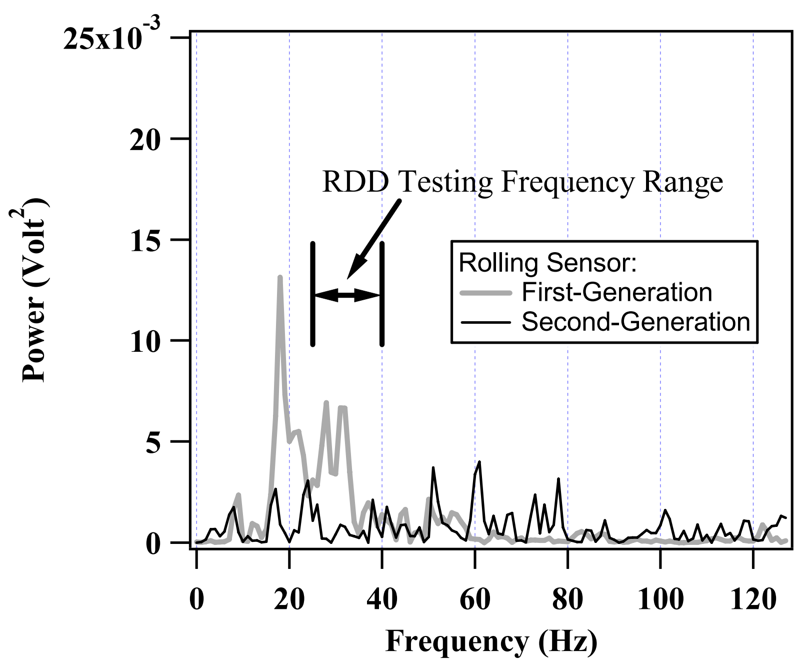

Figure 3.13 Power Spectra of the First-Generation and Second-Generation Rolling Sensors at a Testing Velocity of 3.0 mph (4.5 ft/sec)

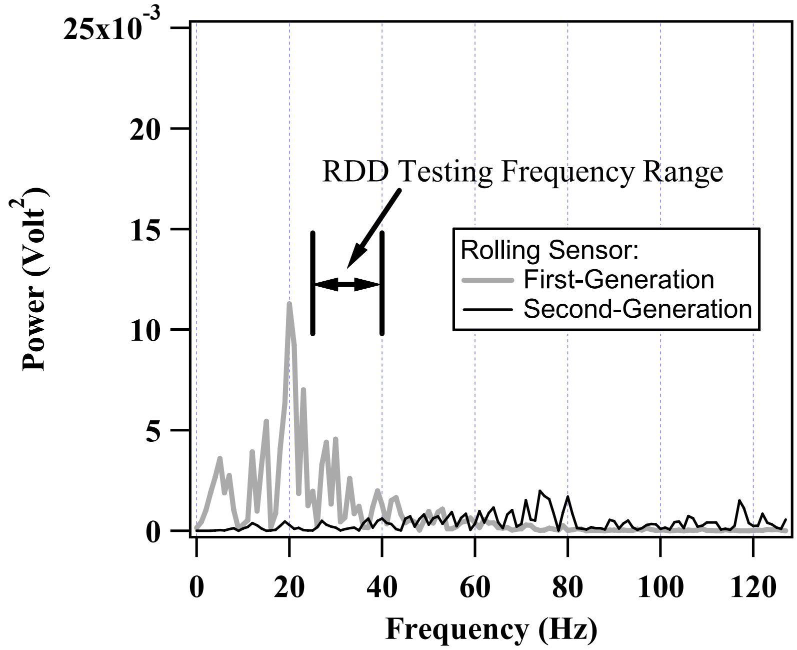

Figure 3.14 Power Spectra of the First-Generation and Second-Generation Rolling Sensors at a Testing Velocity of 3.2 mph (4.7 ft/sec)

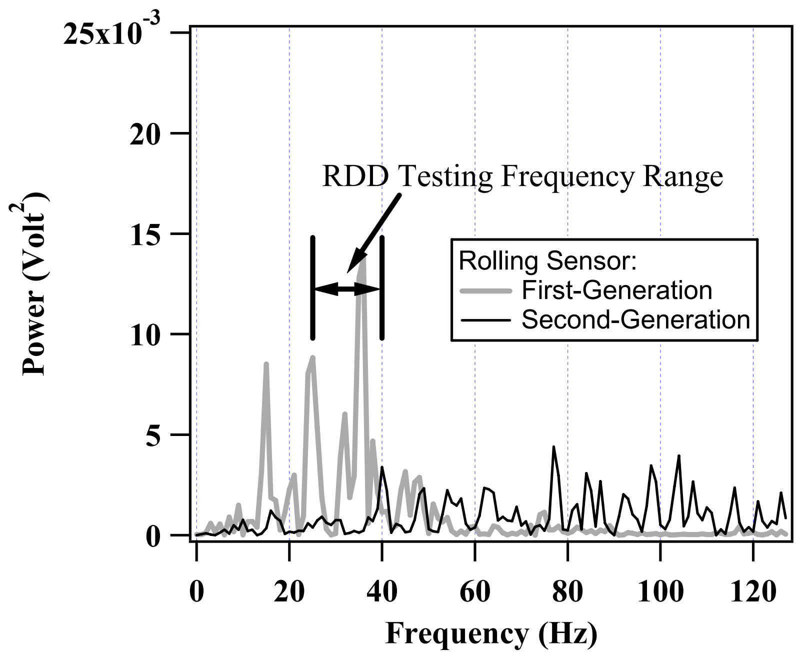

Figure 3.15 Power Spectra of the First-Generation and Second-Generation Rolling Sensors at a Testing Velocity of 3.8 mph (5.6 ft/sec)

3.6 Summary

The rolling sensor used in RDD testing is a contact-type sensor, and the rolling sensor measurement contains both the RDD signal at the operating frequency and noises from different sources. Both the level of rolling noise and the frequency content of the rolling noise is important to the accuracy of RDD deflection measurement. The second-generation rolling sensor built in this project is designed to reduce the level of rolling noise and to avoid having rolling noise concentrated in the RDD operating frequency range. These characteristics have been compared with the first-generation rolling sensor during the preliminary field trials at PRC. These trials have shown that the second-generation rolling sensor reduces the noise level and has a more uniformly distributed rolling noise spectrum than the first-generation rolling sensor. The other critical design aspect that affects the performance of the rolling sensor is the decoupling of the sensor from the pavement. This issue is presented in Chapter 4.

Chapter 4. Field Evaluation of the Second-Generation Rolling Sensor Performance: Decoupling from the Pavement

4.1 Introduction

For the rolling sensor to make accurate measurement of the surface deflection, the rolling sensor needs to stay coupled with the pavement surface. Decoupling is a critical design aspect for the rolling sensor to operate at 3 mph (4.8 km/hr). In this chapter, the governing equation which controls the maximum theoretical testing velocity is first presented. Discussion on the decoupling performance of the second-generation rolling sensor is then presented. Based on the acceleration time histories of the first-generation and second-generation rolling sensors collected during the preliminary field trials at PRC, it was found that the second-generation rolling sensor maintained coupling with the pavement surface at speeds over 3 mph (4.8 km/hr).

4.2 Maximum Theoretical Testing Velocity

A simple model was proposed by Bay et al. (1998) to describe the motion of a rigid wheel rolling over a vertical obstacle. This model assumes the rolling wheel travels in a circular arc path which approximates a parabolic arc with constant acceleration. A diagram of a rigid wheel rolling over a high point with a circular arc path is shown in Figure 4.1. This model assumes that the vertical acceleration is only related to the radius of the rolling wheel and the rolling velocity. With the assumption that the height (h) of the obstacle is small in comparison with the radius (r) of the rigid wheel, the contact problems are independent of the pavement roughness.

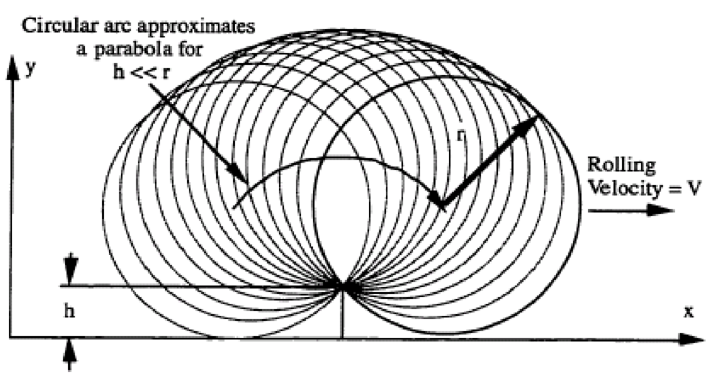

Figure 4.1 Wheel Rolling over a High Point with a Circular Arc Path (from Bay et al., 1998)

The equation which governs the vertical acceleration of a rolling wheel can be calculated using:

$$\frac{\partial^2 y}{\partial t^2} = \frac{-1}{r} V^2 \tag{4.1}$$

where

$\frac{\partial^2 y}{\partial t^2}$ = the vertical acceleration,
r = the radius of rolling wheel, and
V = rolling velocity.

According to this model, the second-generation rolling sensor with 6-in. (152-mm) radius rolling wheels should experience one half of the negative vertical acceleration that the first-generation rolling sensor with 3-in. (76-mm) radius rolling wheels. The rolling sensor will uncouple from the pavement surface when the force between the rolling sensor and the ground approaches zero. For the first-generation rolling sensor, the only resisting force available is the gravity. This means that the limiting acceleration for the first-generation sensor is -1g. For the second-generation rolling sensor, an additional hold-down force (*massless* hold-down system) was provided in addition to its own gravity force. Therefore, the limiting acceleration for the new sensor can be calculated from:

$$a_l = -\frac{F_{hold-down}}{W_{sensor}} - 1g \tag{4.2}$$

where

a_l	=	limiting acceleration
$F_{hold-down}$	=	hold down force
W_{sensor}	=	weight of the rolling sensor

The maximum testing velocity of a rolling sensor is the speed that theoretically the acceleration of the rolling sensor would nearly exceed the allowable hold-down acceleration provided by the self weight of the rolling sensor plus any additional hold-down force. A number of parameters affect the maximum testing velocity (V_{max}). These parameters are:

(1) rolling sensor wheel radius (r)
(2) peak vertical pavement displacement ($v_{p,max}$)
(3) RDD operating frequency (f_o)
(4) hold-down force (F_{hd})
(4) rolling sensor weight (W_{sensor})

The governing equation (after Bay et al., 1998) of the maximum testing velocity is:

$$\frac{1}{r}V^2 + v_{p\max}(2\pi f_O)^2 \le \left(1 + \frac{F_{hd}}{W_{sensor}}\right)g \tag{4.3}$$

where

g = acceleration of gravity

For different rolling sensor designs, the relationships between the maximum testing velocity and the RDD operating frequency are obtained by substituting the rolling sensor wheel radius, weight of the rolling sensor, and the hold-down force into Equation 4.3. A set of such curves are shown in Figure 4.2, which represents the maximum testing speed (V_{max}) that a rolling sensor can theoretically achieve for a pavement that creates $v_{p,max}$ equal to 4 mils (0.10 mm). A value of $v_{p,max}$ of 4 mils is chosen because this is a deflection value that a concrete interstate highway could be expected to have. The hold-down force on each second-generation rolling sensor is expressed in Figure 4.2 by a pressure, with a 35-lb hold-down force applied by the air spring when it is pressurized to 5 psi (34.5 kPa).

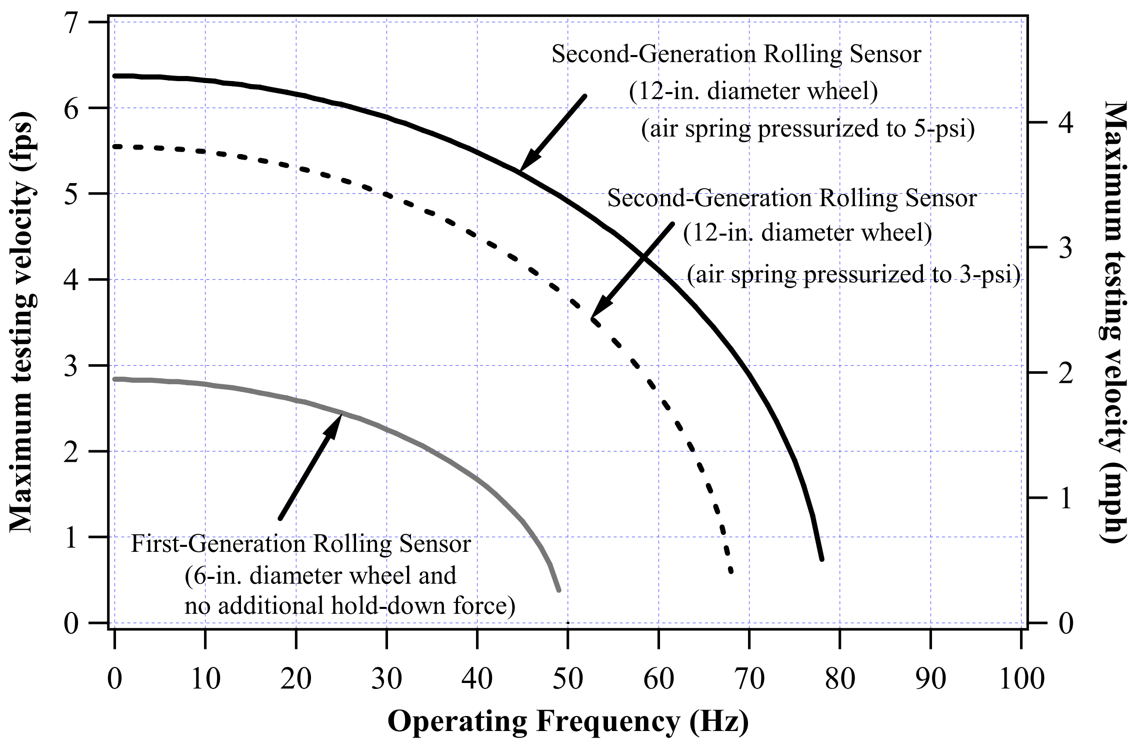

Figure 4.2 Relationships between Maximum Testing Velocity and the RDD Operating Frequency (for $v_{p,\,max}$ = 4 mils, and rolling wheel diameter = 6 in.)

4.3 Maintaining Coupling of Rolling Sensor and Pavement

For the RDD rolling sensor to measure the dynamic deflection of the pavement surface correctly, the rolling sensor has to stay in contact with the pavement surface at all times. As discussed in the previous section, the application of an additional hold-down force helps the second-generation rolling sensor to stay in contact with the pavement surface, which in turn allows the RDD to operate at a faster testing speed. When the rolling sensor exceeds a certain acceleration level, uncoupling will occur.

There are a number of approaches that can be used to ensure the rolling sensor couples with the pavement surface during RDD testing. In the first approach, the acceleration time histories of the rolling sensor are readily available by differentiating the velocity time histories measured by the geophone. This process involves first converting the velocity time histories from the time domain to the frequency domain. Calibration factors are then applied in the frequency domain, and then an Inverse Fast Fourier Transform (IFFT) is used to convert the signal back to the time domain with the units of velocity. The acceleration time history is then obtained by differentiating the velocity time history. In the second approach, an accelerometer can be attached to the body of the rolling sensor. This allows direct measurement of the acceleration time history. An accelerometer with good response in the low frequency range should be selected in this case.

There is a third approach that could be used to evaluate decoupling of the rolling sensor from the pavement. A load cell could be used to measure the contact force between each rolling wheel and the pavement surface. When the rolling sensor decouples from the pavement surface, a sudden drop in the force would be measured.

4.4 Sensor Decoupling Evaluation: Preliminary Field Trials without the RDD Truck

For a second-generation rolling sensor, when the air spring is pressurized at 5 psi (34.5 kPa), it is equivalent to applying a hold-down force of 35 lb (15.9 kg). With the weight of the second-generation rolling sensor being 23 lb (10.5 kg), and assuming a $v_{p,max}$ of 4 mils, the limiting acceleration will be around -2.0g using Equation 4.3. Similarly, the limiting negative vertical acceleration for the first-generation rolling sensor is -0.5g. The measured acceleration time histories for both generations of rolling sensors being tested at different testing speeds are shown in Figures 4.3 to 4.8. The maximum vertical accelerations were obtained using the first approach, which was discussed in Section 4.3. The maximum vertical accelerations measured are summarized for the first-generation and second-generation rolling sensor in Figures 4.9(a) and 4.9(b), respectively.

From Figures 4.3 to 4.8, it can be seen that the second-generation rolling sensor maintains coupling with the pavement at a speed up to approximately 4.5 ft/sec (3 mph). This is a significant improvement when compared with the first-generation rolling sensor which decouples from the pavement at a speed around 2 ft/sec (1.4 mph). Figure 4.9 clearly shows that the second-generation rolling sensor performs properly at speeds around and above 3 mph (4.8 km/hr).

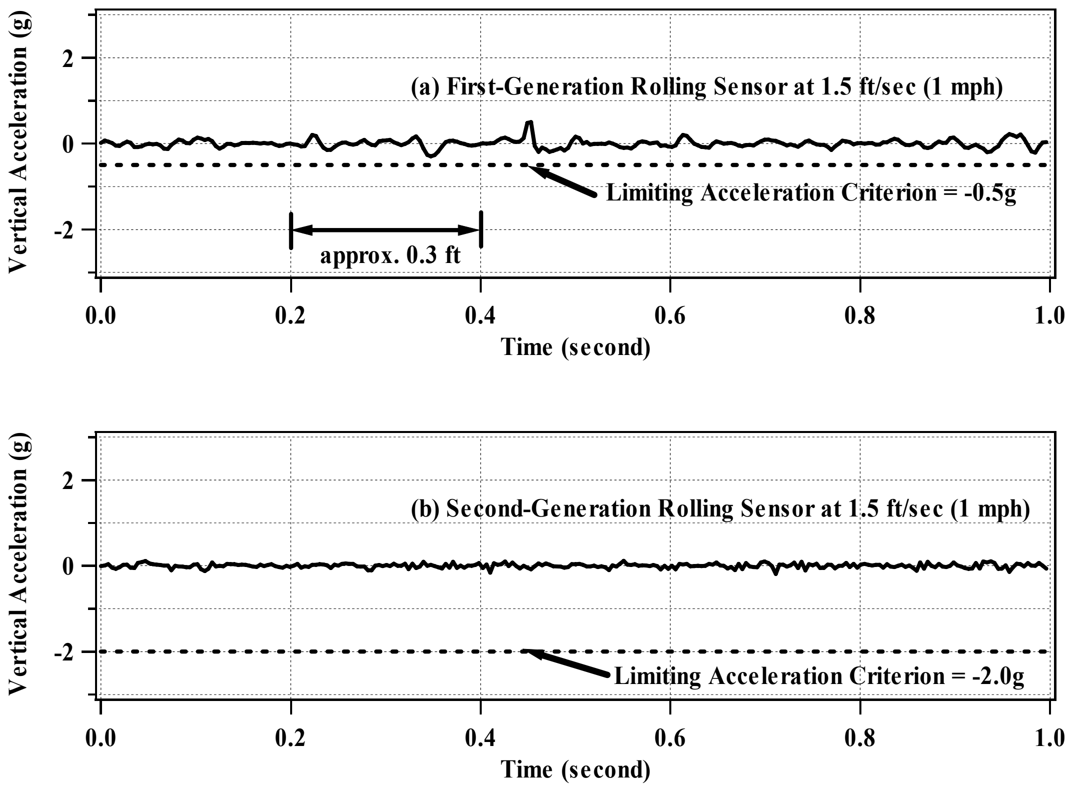

Figure 4.3 (a) and (b). Acceleration Time Histories for First-and Second-Generations Rolling Sensor: Average Speed of 1.5 ft/sec (1 mph)

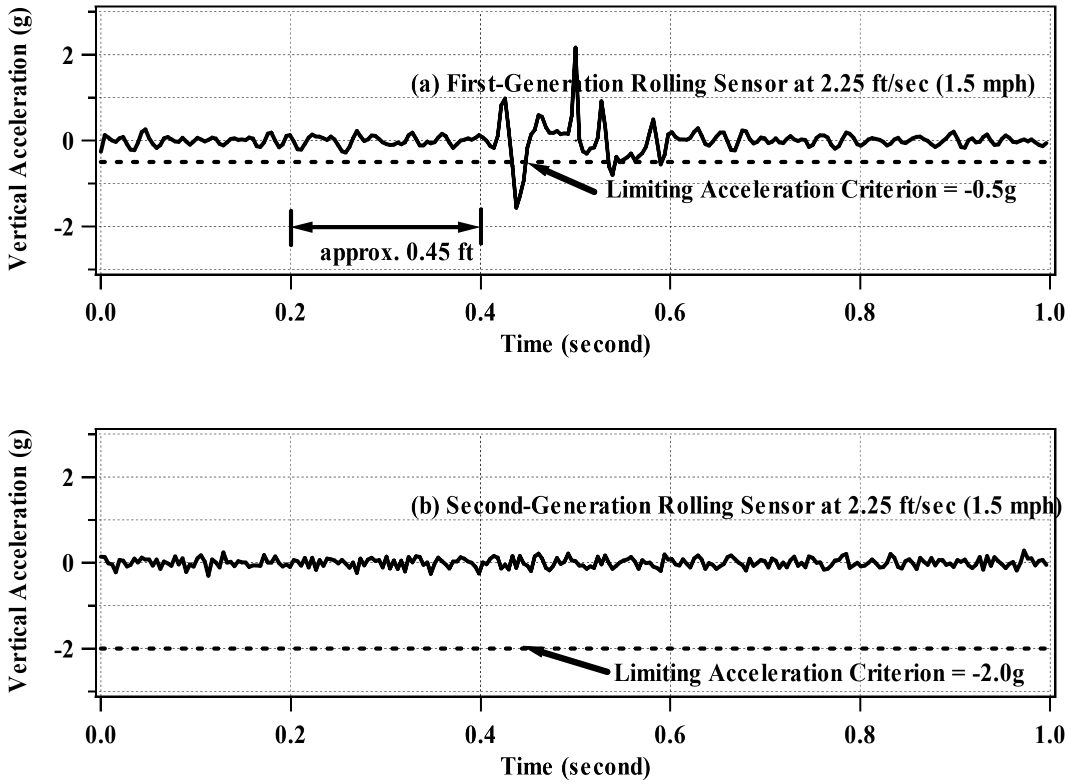

Figure 4.4 (a) and (b). Acceleration Time Histories for First-and Second-Generations Rolling Sensor: Average Speed of 2.25 ft/sec (1.5 mph)

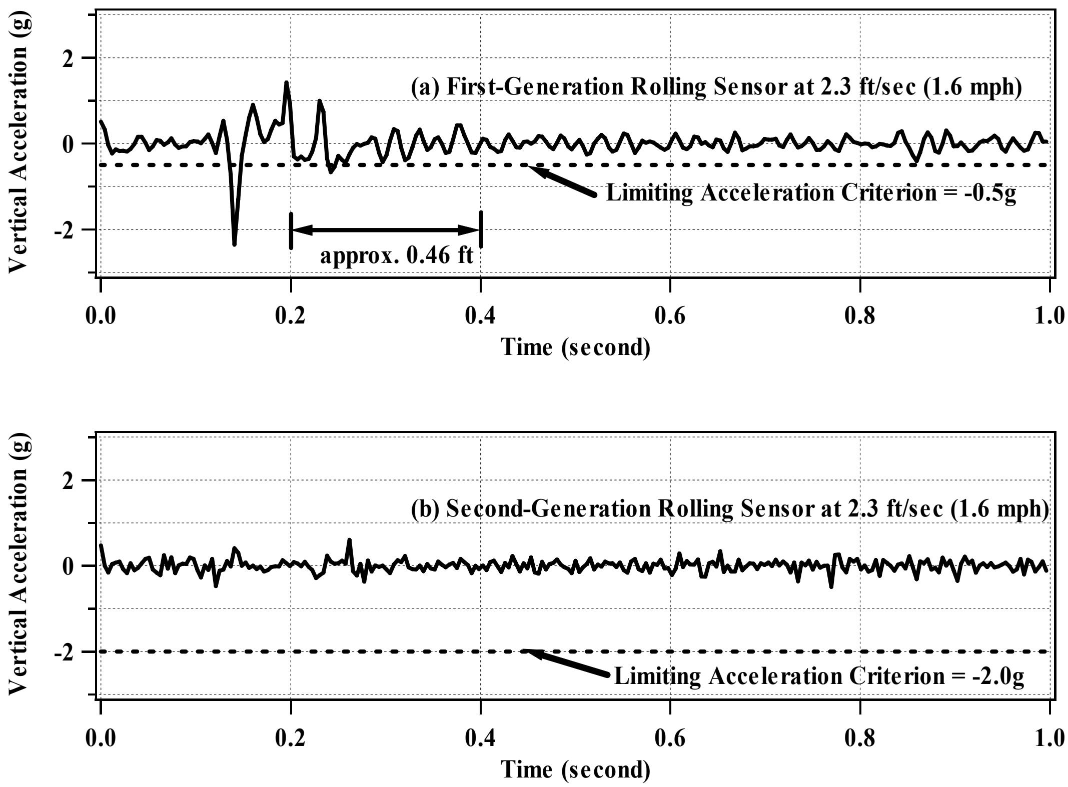

Figure 4.5 (a) and (b). Acceleration Time Histories for First-and Second-Generations Rolling Sensor: Average Speed of 2.3 ft/sec (1.6 mph)

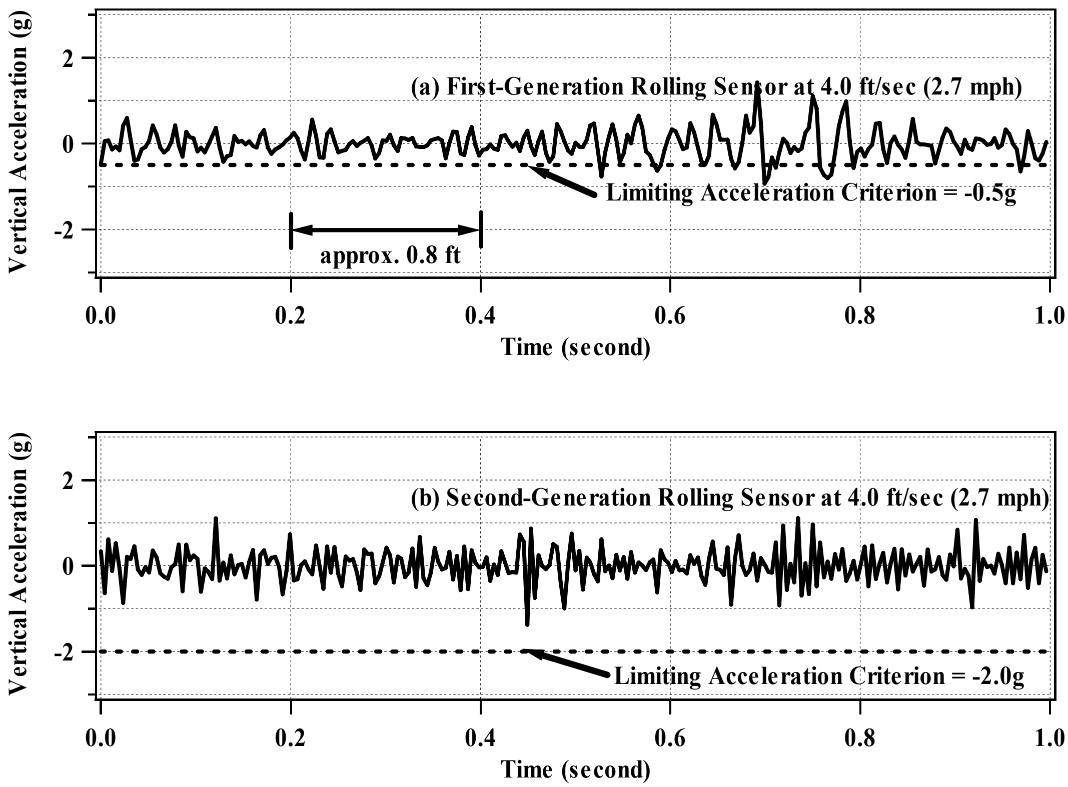

Figure 4.6 (a) and (b). Acceleration Time Histories for First-and Second-Generations Rolling Sensor: Average Speed of 4.0 ft/sec (2.7 mph)

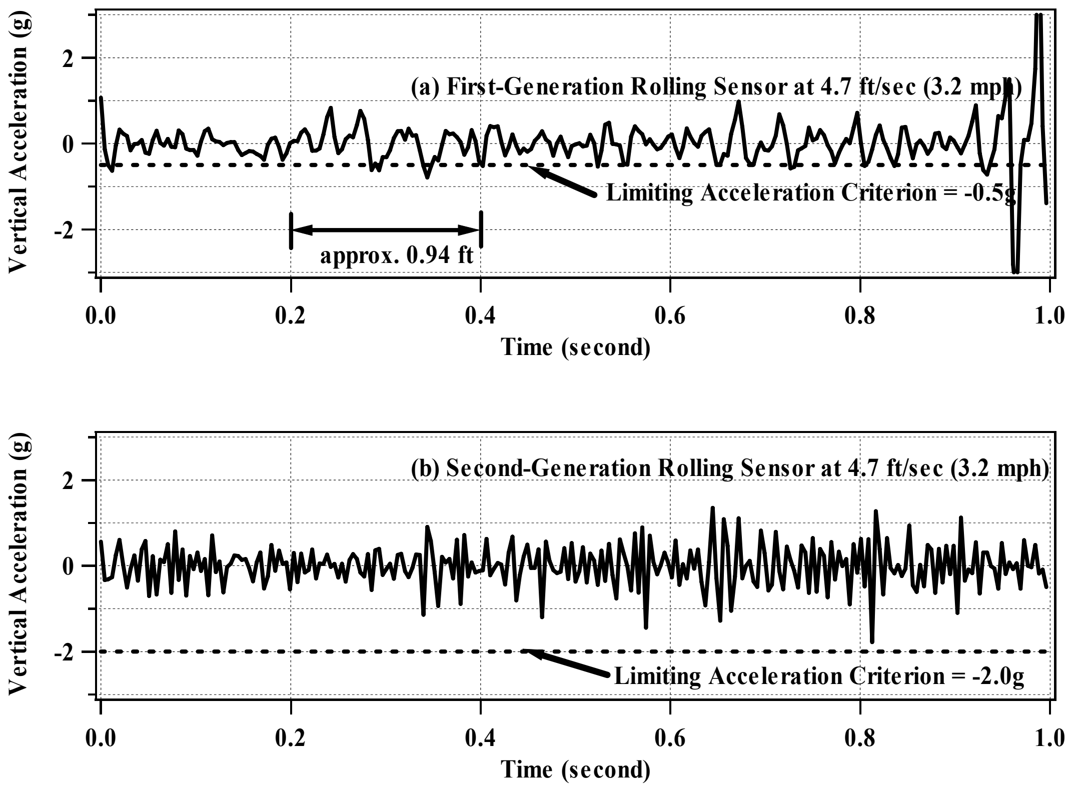

Figure 4.7 (a) and (b). Acceleration Time Histories for First-and Second-Generations Rolling Sensor: Average Speed of 4.7 ft/sec (3.2 mph)

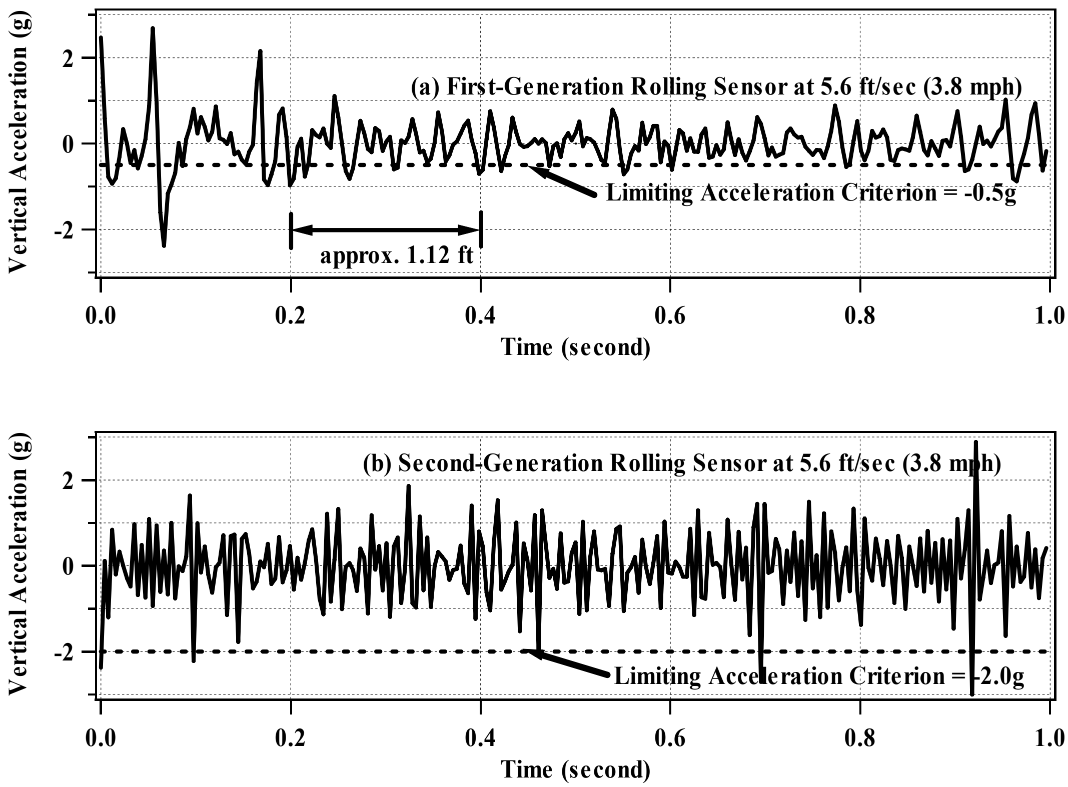

Figure 4.8 (a) and (b). Acceleration Time Histories for First-and Second-Generations Rolling Sensor: Average Speed of 5.6 ft/sec (3.8 mph)

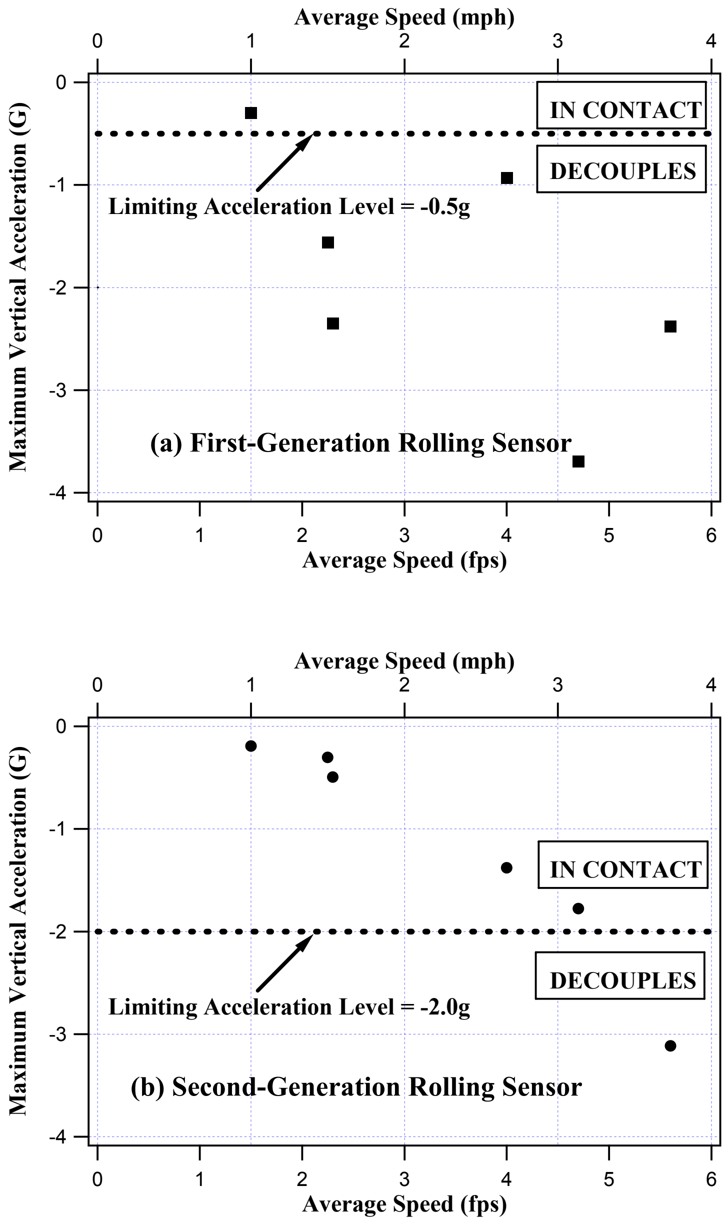

Figure 4.9 (a) and (b). Comparison of the Maximum Vertical Accelerations Between the First-Generation and Second-Generation Rolling Sensors Measured During Rolling-Noise Field Trials

4.5 Summary

In this chapter, the decoupling performance of the first-and second-generation rolling sensors was compared using data collected in the preliminary field trials at PRC. It was found that the second-generation rolling sensor maintains coupling with the pavement at speeds above and around 3 mph (4.8 km/hr).

Chapter 5. Field Trials with Complete RDD System

5.1 Introduction

Field trials were performed at the Texas Accelerated Pavement Testing (TxAPT) site at PRC using the RDD. Continuous deflection profiles using the first-generation and second-generation rolling sensors were collected at different testing speeds. These deflection profiles are presented in this chapter to demonstrate the ability of the RDD to collect continuous deflection profile at testing speed around 3 mph (4.8 km/hr) using the newly developed second-generation rolling sensor.

5.2 Field Trials with Complete RDD System—TxAPT Site at PRC

On October 23, 2005, field trials were performed on the shoulder lane of the TxAPT site at PRC. A photograph of the RDD testing on the TxAPT site is shown in Figure 5.1. Continuous deflection profiles were collected using the second-generation rolling sensor at different testing speeds. Deflection profiles that were collected at an average test velocity of 1, 2, and 3 mph (1.6, 3.2, and 4.8 km/hr) are shown in Figure 5.2. The average temperature of the AC pavement surface was about 35^{o} C when the three deflection profiles were collected. The three deflection profiles compare well, in terms of absolute deflections and in terms of trends.

A continuous deflection profile was also collected with the first-generation rolling sensor at the TxAPT site in the early morning of October 23, 2005. This deflection profile has lower values than the other three collected using the second-generation rolling sensor. The pavement surface temperature was 19.6^{o} C. In this case, the pavement was slightly cooler and the lower deflections are attributed to the lower temperature. Therefore, to compare the measurement between the first- and second- generation rolling sensors, a surface temperatures correction factor has to be applied to each deflection profile before the different deflection profiles can be compared. The procedure used to correct for the temperature differences in each deflection profile is as follows: (1) plot the deflection value collected at different runs with the surface temperature, as shown in Figure 5.3, (2) perform a linear regression analysis to determine the relationship between the deflection and the measured surface temperatures, and (3) apply the temperature correction factor to each deflection profile to a temperature of 35^{o} C. The four temperature-corrected deflection profiles are shown in Figure 5.4. In this case, all four deflection profiles compared well, both in trends and absolute deflections. The results showed that the second-generation rolling sensor meets the goal of performing well at a testing speed of 3 mph (4.8 km/hr).

Figure 5.1 Photograph of RDD Testing on the Shoulder of the TxAPT Site

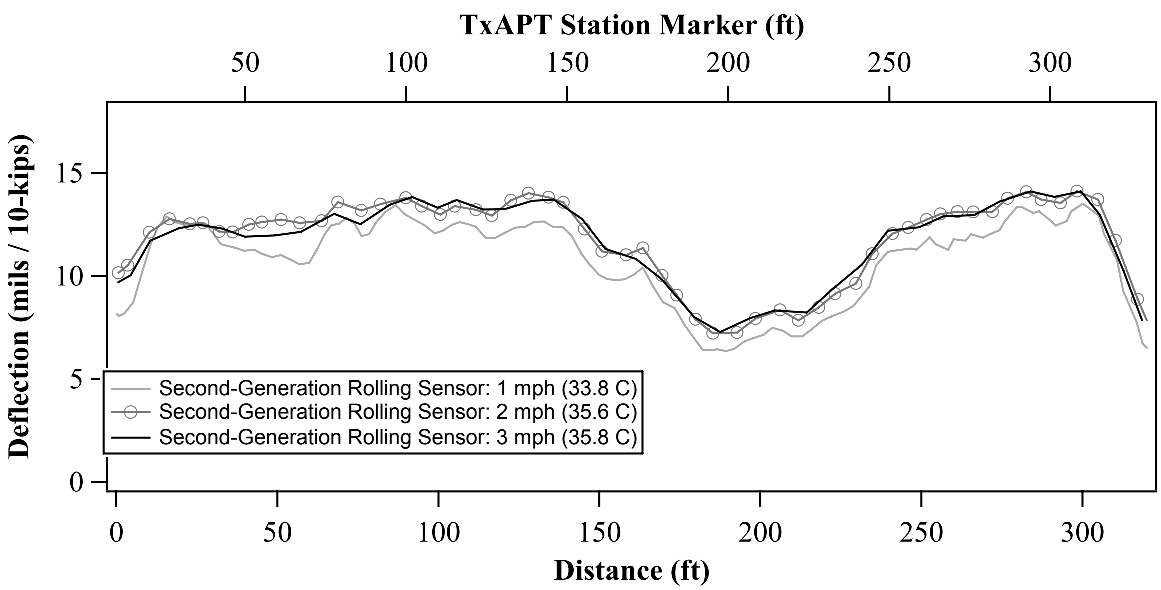

Figure 5.2 RDD Continuous Deflection Profiles Collected Using the Second-Generation Rolling Sensor (Without Temperature Correction)

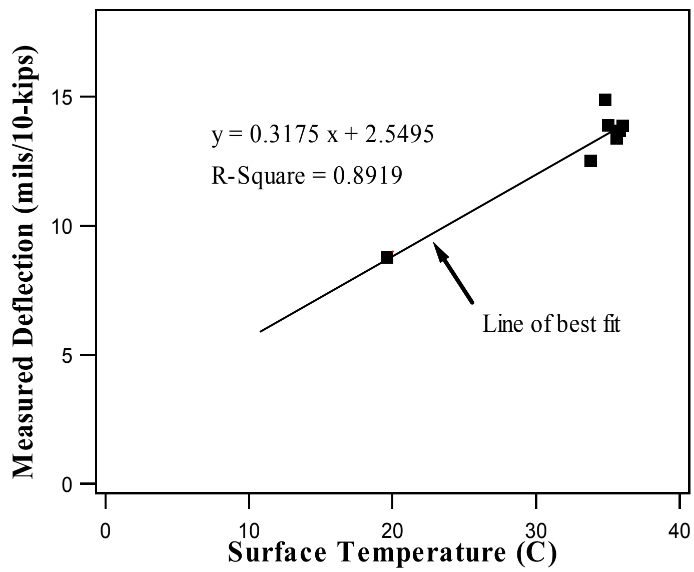

Figure 5.3 Temperature Correction Relationship

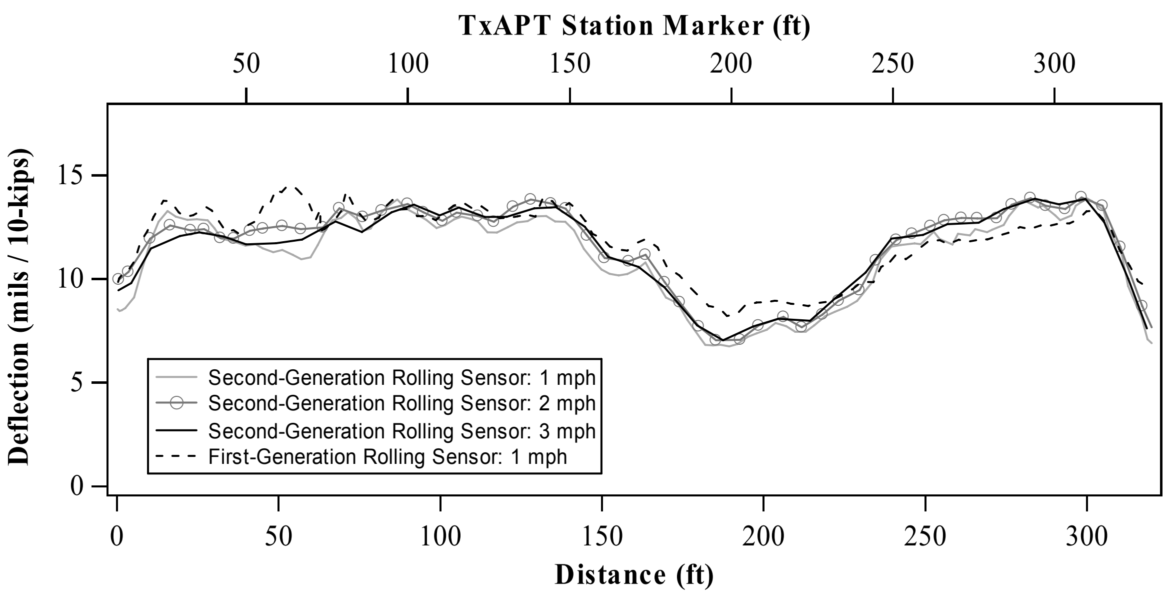

Figure 5.4 RDD Continuous Deflection Profiles Collected Using the Second-Generation Rolling Sensor (After Temperature Correction)

5.3 Summary

Based on the continuous deflection profiles collected at the TxAPT site, it was shown that the second-generation rolling sensor can readily collect deflection profiles at a testing speed of 3 mph (4.8 km/hr). Also, this deflection profile compares well with the deflection profiles that were collected at different speeds. It should be noted that the deflection profiles presented in this chapter were collected at the TxAPT site, which is a smooth and untrafficked flexible pavement. More understanding of the performance of the second-generation rolling sensors on in-service pavements can be gained by running field trials on future TxDOT project-level studies that have a range of pavement types and roughnesses.

Chapter 6. Summary, Conclusions, and Recommendations

6.1 Summary

The current testing speed of the RDD is around 1 mph (1.6 km/hr). At this speed, the RDD crews are exposed to the hazardous high-speed traffic environment for significant periods of time. To reduce the exposure time and to increase the cost efficiency of testing, TxDOT Research Project 0-4357 was initiated with the goal of increasing the current testing speed of the RDD. The primary element that limits the current testing speed to around 1 mph (1.6 km/hr) is the current design of the rolling sensors. These sensors have performed well over the last decade and have been used on numerous project-level studies dealing with highway and airport pavements. The 1-mph (1.6 km/hr) rolling sensor is referred to as the first-generation rolling sensor throughout this project.

Under TxDOT Research Project 0-4357, four second-generation rolling sensors have been designed and built. The second-generation rolling sensor was built to accomplish two objectives. These objectives are:

(1) allow the current RDD test speed to increase to around 3 mph (4.8 km/hr), and
(2) reduce the measured rolling noise.

During the design of the second-generation rolling sensor, various design considerations were considered as discussed in Chapter 2. The main features incorporated into the second-generation rolling sensor are as follows: (1) an additional hold-down force is provided by a pressurized air spring located at the top of each rolling sensor. This additional hold-down force allows the rolling sensor to stay coupled with the pavement surface when tested at speeds up to 3 mph (4.8 km/hr); (2) larger diameter rolling wheels are used to reduce the negative vertical acceleration and the level of rolling noise within the RDD measurement.

The performance of the second-generation rolling sensor was presented in Chapter 3 in terms of rolling noise. It was found that the second-generation rolling sensor has a lower rolling-noise level than the first-generation rolling sensor. Then the rolling sensor was evaluated in terms of its decoupling performance in Chapter 4. It was found that the second-generation rolling sensor stays coupled with the pavement at speeds over 3 mph (4.8 km/hr). Overall performance of the sensor was also evaluated in Chapter 5 by collecting continuous deflection profile at the TxAPT site. Based on two testing trials performed at PRC, it was found that the second-generation rolling sensor can readily achieve a testing speed of 3 mph (4.8 km/hr). Even though the field trials were collected at the TxAPT site, which is a smooth and untrafficked flexible pavement, more trials using the second-generation rolling sensors on in-service pavements should be carried out to understand the performance of the rolling sensors. In these trials, it was clearly shown, however, that the second-generation rolling sensor has less rolling noise when compared with the first-generation rolling sensor, which represents an important improvement in the evolution of the RDD.

6.2 Conclusions

Under TxDOT Research Project 0-4357, four second-generation rolling sensors were designed, built and calibrated in the laboratory. It was found from field trials that the second-generation rolling sensor can collect continuous deflection profiles at a testing speed of 3 mph (4.8 km/hr). This increase in speed triples the current maximum RDD testing speed of 1 mph (1.6 km/hr) and is a major improvement to the productivity of the RDD testing device.

The second-generation rolling sensor also has less rolling noise than the first-generation rolling sensor when tested at the same speed. As a result, a more accurate RDD deflection profile can be obtained by having less rolling noise within the RDD measurement.

6.3 Recommendations

A working design of the second-generation rolling sensor has been developed under this research project. However, due to the space limitation under the RDD truck, the current towing frame arrangement is not yet ready for implementation in the field. A towing frame needs to be designed which would have the following characteristics:

(1) Position the second-generation rolling sensors at locations where the deflection basin is measured

(2) Sufficient self weight to provide the reaction force required by each air spring

(3) Self raising and lowering mechanical system which would minimize the installation time of the rolling sensors in the field

References

Bay, J. A., and Stokoe, K. H., II, "Development of a Rolling Dynamic Deflectometer for Continuous Deflection Testing of Pavements," CTR Report 1422-3F, The University of Texas at Austin, May 1998.

Richart, F. E., Jr., Hall, J. R., Jr., and Woods, R. D., "Vibration of Soils and Foundations," Prentice-Hall, Inc., Englewood Cliffs, New Jersey.

ERES Consultants, "Rolling Wheel Deflectometer (RWD) Demonstration and Comparison to Other Devices—Final Report," Champaign, Illinois, February 2004.